



Stable Tuna Mercury Concentrations since 1971 Illustrate Marine Inertia and the Need for Strong Emission Reductions under the Minamata Convention

Anaïs Médieu, David Point, Jeroen Sonke, Hélène Angot, Valérie Allain, Nathalie Bodin, Douglas Adams, Anders Bignert, David Streets, Pearse Buchanan, et al.

► To cite this version:

Anaïs Médieu, David Point, Jeroen Sonke, Hélène Angot, Valérie Allain, et al.. Stable Tuna Mercury Concentrations since 1971 Illustrate Marine Inertia and the Need for Strong Emission Reductions under the Minamata Convention. *Environmental Science and Technology Letters*, 2024, 11 (3), pp.250-258. 10.1021/acs.estlett.3c00949 . hal-04508967

HAL Id: hal-04508967

<https://hal.science/hal-04508967v1>

Submitted on 1 Dec 2024

HAL is a multi-disciplinary open access archive for the deposit and dissemination of scientific research documents, whether they are published or not. The documents may come from teaching and research institutions in France or abroad, or from public or private research centers.

L'archive ouverte pluridisciplinaire **HAL**, est destinée au dépôt et à la diffusion de documents scientifiques de niveau recherche, publiés ou non, émanant des établissements d'enseignement et de recherche français ou étrangers, des laboratoires publics ou privés.

Stable tuna mercury concentrations since 1971 illustrate marine inertia and the need for strong emission reductions under the Minamata Convention

Anaïs Médieu¹, David Point², Jeroen E. Sonke², Hélène Angot³, Valérie Allain⁴, Nathalie Bodin⁵, Douglas H. Adams⁶, Anders Bignert⁷, David G. Streets⁸, Pearse B. Buchanan⁹, Lars-Eric Heimbürger-Boavida¹⁰, Heidi Pethybridge¹¹, David P. Gillikin¹², Frédéric Ménard¹⁰, C. Anela Choy¹³, Takaaki Itai¹⁴, Paco Bustamante¹⁵, Zahrah Dhurmeea¹, Bridget E. Ferriss¹⁶, Bernard Bourlès¹⁷, Jérémie Habasque¹, Anouk Verheyden¹², Jean-Marie Munaron¹, Laure Laffont², Olivier Gauthier¹, Anne Lorrain¹

¹IRD, Univ Brest, CNRS, Ifremer, LEMAR, IUEM, F-29280 Plouzane, France

²Observatoire Midi-Pyrénées, GET, UMR CNRS 5563/IRD 234, Université Paul Sabatier Toulouse 3, Toulouse, France

³Univ. Grenoble Alpes, CNRS, INRAE, IRD, Grenoble INP, IGE, Grenoble, France

⁴Pacific Community, Oceanic Fisheries Programme, Nouméa, New-Caledonia

⁵Sustainable Ocean Seychelles (SOS), BeauBelle, Mahé, Seychelles

⁶Florida Fish and Wildlife Conservation Commission, Fish and Wildlife Research Institute, Melbourne FL, 32901, USA

⁷Department of Environmental Research and Monitoring, Swedish Museum of Natural History (NRM), SE-104 05 Stockholm, Sweden

⁸Harvard John A. Paulson School of Engineering and Applied Sciences, Cambridge, Massachusetts

⁹University of Carnegie, Department of Global Ecology, Stanford, California, 94305, USA.

¹⁰Aix Marseille Univ., CNRS/ISU, IRD, Univ. de Toulon, Mediterranean Institute of Oceanography (MIO), Marseille, France

¹¹CSIRO Environment, Hobart, Tasmania, Australia

¹²Department of Geosciences, Union College, 807 Union St., Schenectady, NY, 12308, USA

¹³Scripps Institution of Oceanography, University of California San Diego, La Jolla, California 92037, USA

¹⁴Department of Earth and Planetary Sciences, Graduate School of Science, The University of Tokyo, Bunkyo-Ku, Tokyo, 113-0033, Japan

¹⁵Littoral Environnement Société (LIENSs), UMR 7266-CNRS, La Rochelle Université, 2 rue Olympe de Gouges, 17000 La Rochelle, France

¹⁶Resource Ecology and Fisheries Management Division, Alaska Fisheries Science Center, National Marine Fisheries, NOAA, Seattle, Washington, USA

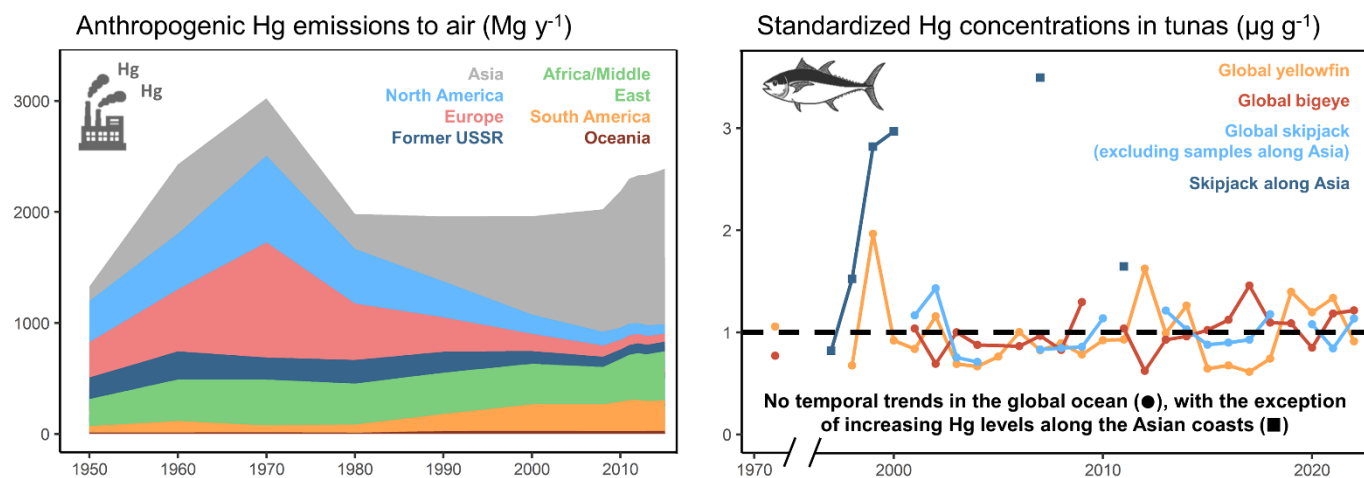
¹⁷IRD, IMAGO, Plouzané, France

Abstract

Humans are exposed to toxic methylmercury mainly by consuming marine fish. While reducing mercury emissions and releases aims to protect human health, it is unclear how this affects methylmercury concentrations in seawater and marine biota. We compiled existing and newly acquired mercury concentrations in tropical tunas from the global ocean to explore multidecadal mercury variability between 1971 and 2022. We show the strong inter-annual variability of tuna mercury concentrations at the global scale, after correcting for bioaccumulation effects. We found increasing mercury concentrations in skipjack in the late 1990s in the northwestern Pacific, likely resulting from concomitant increasing Asian mercury emissions. Elsewhere, stable long-term trends of tuna mercury concentrations contrast with an overall decline in global anthropogenic mercury emissions and deposition since the 1970s. Modeling suggests that this limited response observed in tunas likely reflects the inertia of surface ocean mercury with respect to declining emissions, as it is supplied by legacy mercury that accumulated in the subsurface ocean over centuries. To achieve measurable declines in mercury concentrations in highly consumed pelagic fish in the near future, aggressive emission reductions and long-term and continuous mercury monitoring in marine biota are needed.

Keywords: methylmercury, yellowfin, bigeye, skipjack, global temporal heterogeneity, anthropogenic emissions, legacy mercury, Minamata Convention.

Graphical abstract



Introduction

Mercury (Hg) is a widespread contaminant that can be naturally converted into methylmercury (MeHg) in marine ecosystems^{1,2}. Methylmercury is associated with neurocognitive deficits in human foetuses and children, and with cardiovascular effects in adults^{3,4}. Humans are exposed to MeHg mainly by the consumption of seafood, and tunas in particular, which are amongst the most consumed marine fish worldwide⁵, and have relatively high MeHg concentrations^{6–8}. Global health impacts associated with MeHg exposure for the general population are estimated at \$117 billion per year⁹. To protect human health and the environment from harmful effects, the United Nations Environment Programme Minamata Convention entered into force in 2017 with the objective of reducing anthropogenic Hg emissions.

Most anthropogenic Hg releases are estimated to have occurred during the last five centuries¹⁰. Cumulative releases to the atmosphere have been largest in North America and Europe, yet anthropogenic emissions and deposition in these two regions have declined since the 1970s, following emission reduction measures. Conversely, anthropogenic Hg releases in Asia have increased since the 1980s¹¹. Anthropogenic Hg uses and emissions have considerably modified the natural global Hg cycle^{12,13}. In the atmosphere, higher Hg levels are measured in the northern hemisphere, following the location of the main anthropogenic Hg emissions¹⁴. In the open ocean, total Hg concentrations at depths of 100–1,000 m are thought to have tripled globally¹⁵, yet scarce Hg observation data in seawater suggest contrasted temporal trends^{16,17}. It is still unclear which fraction of anthropogenic Hg is converted into MeHg in seawater and biomagnified in marine biota. While tunas represent a major route of MeHg exposure to humans, temporal studies of their Hg concentrations are limited, showing contrasting temporal trends among species and ocean regions^{18–21}. Understanding and predicting spatial and temporal Hg trends in tunas remains crucial for anticipating changes in human exposure and evaluating the effectiveness of the Minamata Convention in protecting humans who consume seafood.

In this study, we investigate the temporal variability of Hg concentrations in tunas from 1971 to 2022 in six regions of the Pacific, Atlantic, and Indian Oceans. We revisited existing and acquired new Hg data in tropical tunas, i.e., yellowfin (*Thunnus albacares*), bigeye (*T. obesus*), and skipjack (*Katsuwonus pelamis*). These tunas are top predators, globally distributed, highly exploited (constituting 94% of global tuna catches), and hold significant importance for human health⁵. Tropical tunas exhibit distinct foraging habitats (skipjack and yellowfin primarily feeding on epipelagic prey, and bigeye generally rely on mesopelagic species)²², growth rates and lifespan²³. Moreover, all three display relatively limited movements and show site fidelity^{24,25}, compared tunas that undertake large transoceanic migrations^{26–28}. Tropical tunas are thus expected to reflect MeHg patterns in surface and subsurface waters, making them valuable biological sentinel species for exploring various lag times in response to changes in Hg emissions. After standardizing Hg concentrations by tuna length, we reveal overall stable tuna Hg concentrations in the global ocean, except in the northwestern Pacific Ocean where tuna Hg concentrations increased significantly in the late 1990s.

Materials & Methods

Tuna sampling and data compilation

We assembled 2,910 tuna muscle Hg concentrations in six regions of the Pacific, Atlantic and Indian Oceans (Figure 1 and Table S1), allowing temporal analysis covering approximately 50 years from 1971 to 2022, depending on the region. We added 547 tuna Hg concentrations to the dataset of Drevnick and Brooks (2017) (Figure S1), and 37 data points to that of Médieu et al. (2021) to re-evaluate the previously identified increasing and stable tuna Hg concentrations in the central north and southwestern Pacific Ocean, respectively. In the northwestern Atlantic Ocean, where decreasing Hg concentrations were observed in Atlantic bluefin between 2004 and 2012²⁰, we examined the temporal variability of Hg concentrations in yellowfin between 1999 and 2011. Our global compilation extends to regions such as the western Indian, the northwestern Pacific, and the eastern equatorial Atlantic, where no temporal Hg data in tunas have been available to date.

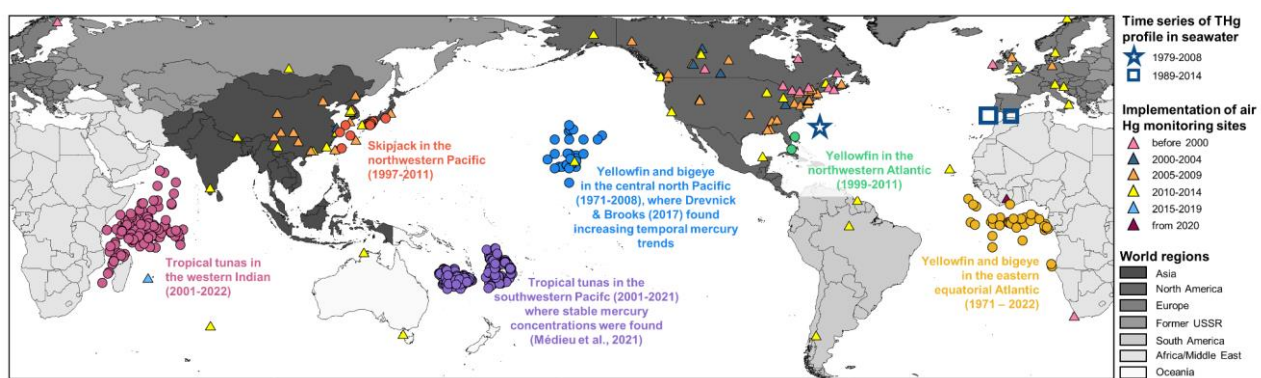


Figure 1. Origin of the tropical tuna samples. The temporal variability of mercury (Hg) concentrations was investigated in tropical tunas sampled in six regions of the global ocean. Coloured dots represent tuna catch locations, while coloured triangles show air monitoring sites according to their starting year. The blue star and squares represent the three locations where seawater concentrations profiles of total mercury (THg) are available in multiple years^{16,17}. Countries are coloured following the definition of the seven world regions in the emissions inventory of Streets et al.^{10,11,29,30}.

Total mercury concentrations and ecological tracer analyses in tunas

Total Hg concentrations were measured in tuna muscle samples in different study-specific laboratories, with laboratory-specific reference standards to ensure accuracy and traceability, and allow comparison of regional datasets. The total Hg content is expressed on a dry weight (dw) basis and is considered to reflect MeHg concentration, as most of the total Hg (> 91%) is in its methylated form in tuna white muscle³¹. As Hg is known to bioaccumulate with fish length, we calculated length-standardized Hg concentrations to remove the length effect when exploring temporal variability^{8,21,32} (Figure S2).

To account for possible confounding temporal changes in tuna trophic ecology, in particular to investigate the temporal variability of tuna trophic position, muscle nitrogen ($\delta^{15}\text{N}$) stable isotope values were also compiled globally when possible (i.e., data available for more than two years; n = 1535 (Table S1)). Analytical methods are presented in the Supporting Information.

Temporal seawater concentration profiles, air monitoring sites, emissions to air inventory, and future emissions scenarios

To examine tuna Hg concentrations alongside seawater Hg concentrations, we reviewed the available temporal concentrations profiles of total Hg in seawater (Figure 1). Similarly, air monitoring sites measuring atmospheric Hg concentrations around the globe were compiled from the literature (Figure 1 and Table S2) to explore tuna Hg data alongside atmospheric Hg concentrations. Moreover, mean anthropogenic Hg emission estimates to the atmosphere per decade for the period 1970-2010, and annually for the period 2010-2015, were taken from the emission inventory of Streets et al.^{10,11,29,30}. This emission inventory discerns several world regions (Figure 1), and includes 17 source categories.

We used a box model^{33,34} to simulate the influence over time of global anthropogenic emissions on Hg masses in the atmosphere, surface ocean, subsurface ocean, and deep ocean. The model was driven by 2000 BCE to 2015 CE primary anthropogenic emissions from Streets et al.^{10,11,29,30}. To simulate future emissions (2016-2100), we considered three emissions scenarios^{35,36}: i) a current policy scenario, ii) a more stringent new policy scenario, and iii) a maximum feasible reduction scenario that leads to a dramatic decrease of annual Hg emissions (see also the supporting information).

Results & discussion

Standardized tuna mercury concentrations

Tuna Hg concentrations were highly variable among years globally when MeHg bioaccumulation with tuna length was accounted for. Significant temporal trends of Hg levels were evidenced in only skipjack along the Asian coasts. Hg concentrations in 1997 and 1998 were significantly lower than in 1999, 2000, and 2007, suggesting an increase of skipjack Hg concentrations at the end of the 1990s in the northwestern Pacific (Figure 2C and Table S3C). Skipjack Hg concentrations in the same area in 2011 were significantly lower than in 1999, 2000, and 2007 but comparable to those in the earliest years, which suggests a decrease in skipjack Hg concentrations in the 2010s, although more recent data would be necessary to validate this result. Elsewhere, in all regions, our comparative approach reveals that tuna Hg concentrations remained stable over each study period, as no significant difference between old and recent data was found (Figure 2A,B,G-L and Table S3A,B,G-I).

This apparent stability of tuna Hg concentrations over multiple decades in all regions, except for skipjack in the northwestern Pacific, is consistent with the reported stable tuna Hg concentrations over the past two decades in the southwestern Pacific²¹, confirmed here with new data in 2020 and 2021 (Figure 2D-F and Table S3D,E). Our results align with previously observed stable Hg concentrations in yellowfin in the central north Pacific, upon comparison of data from 1971 and 1998.³⁷ However, they diverge from more recent reports indicating increasing trends in yellowfin ($n = 5$ years) and bigeye ($n = 4$ years) during the period of 1998–2008.¹⁹ These discrepancies result from our larger data set (547 data points added to the initial 422 observations), which encompasses an additional year and broader ranges of fish sizes and Hg concentrations (Figure S1). In the northwestern Atlantic, stable Hg concentrations in yellowfin contrast with the reported mean annual decrease of 2.4% between 2004 and 2012 ($n = 9$ years) in bluefin tuna.²⁰ However, our results align with the apparent stability of

bluefin Hg levels in the same region between the 1970s and 2017 when reinvestigated with additional old and recent data points ($n = 13$ years).³⁸ These comparisons highlight the need for collecting long and continuous temporal data on tuna Hg concentrations to be able to justify trend detection in a time series.

All species-specific Hg concentrations were on the same order of magnitude among regions, except for bigeye and skipjack in the southwestern and northwestern Pacific, respectively (Figure 2). Bigeye Hg concentrations in the southwestern Pacific were 2–3 times higher than in other regions, likely associated with the particular marine physical and biogeochemical conditions: a deeper thermocline giving bigeye access to deeper waters and a high peak of dissolved MeHg concentration in subsurface waters fueling the mesopelagic food web.^{8,39} In the northwestern Pacific, skipjack Hg concentrations were up to 3–4 times higher than in the southwestern Pacific and the western Indian (Figure 2C,F,H), likely reflecting a regional anthropogenic Hg contribution from Asia³² (see below).

Comparison with seawater and atmospheric mercury

In the global ocean, only three temporal total Hg concentration profiles in the water column are available to explore the long-term trends of seawater Hg (Figure 1), relying on four sampling years and showing contrasting results.^{16,17} Atmospheric Hg concentrations and deposition are extensively monitored worldwide (Figure 1 and Table S2) and exhibited in Europe a broad 2-fold decrease between 1970 and 1990 as a result of large reductions in anthropogenic emissions in North America and Europe.^{36,40–42} Similarly, trends in Hg deposition inferred from remote peat sediments indicate a synchronous 2-fold decrease across the planet during the late 20th century.⁴³ Nevertheless, we find little spatial and temporal overlap between tuna Hg and atmospheric and marine data, preventing direct comparisons (Figure 1).

Studies of historical primary Hg emissions to air^{10,11,29,30} provide an alternative to the limited local atmospheric observation data to investigate the relationship between tuna Hg trends and atmospheric Hg emissions. The increase in skipjack Hg concentrations in the northwestern Pacific in the late 1990s mirrors increasing Hg emissions to the atmosphere from Asia over the same period (Figure 2C). This suggests a significant contribution to anthropogenic Hg release to marine Hg in this particular region, as already shown in seawater,^{44,45} sediment,⁴⁶ and tuna^{32,47} samples. The decrease in tuna Hg levels after 2011 may reflect the documented reduction in Hg emissions and atmospheric levels in East Asia since the 2010s, and/or changes in emitted Hg speciation in China.^{48–53} The inventory used in our study¹¹ does not reflect these recent changes in emissions (Figure 2C). To gain a more accurate understanding of how changing local anthropogenic Hg emissions affect the marine Hg cycle in this specific region, additional Hg observation data in tunas, seawater, and the atmosphere are needed, along with improved emission inventories.

Elsewhere, stable tuna Hg concentrations between 1971 and 2022 contrast with the significant decrease in global primary anthropogenic Hg emission, concentration, and deposition trends and natural archive-based reconstructed deposition since the 1970s.^{36,40–43} Such contrast has already been documented in other aquatic ecosystems⁵⁴ and likely results from (i) multicausal and local processes (e.g., marine biogeochemistry and tuna ecology) controlling MeHg net production, bioavailability, and biomagnification and (ii) the large amount of legacy Hg, i.e., historically emitted Hg that continues to cycle through biogeochemical compartments and remains available for biouptake, leading to time lags in the biotic response to reductions in primary Hg emission or release. The surface ocean (~0–50 m) is

a small reservoir that is sensitive to changes in Hg loadings from atmospheric deposition, subsurface ocean Hg via upward mixing, and river runoff.³⁴ The subsurface ocean (~50–1500 m) has received large amounts of legacy Hg over several centuries by Hg export from the surface via particle scavenging and mixing. Because of the upward mixing of this legacy Hg, the surface ocean reservoir takes years or decades to respond to changes in primary emissions,^{34,55} as illustrated with new Hg box model simulations forced with updated Hg emissions^{10,11,29,30} (Figure 3). Following the sharp 30% decrease in primary emissions in the 1970s, the Hg mass in the surface ocean only decreased by 2%. Subsequently, it rapidly increased over several decades, driven by legacy Hg from the subsurface ocean, which surpassed atmospheric deposition of Hg to the surface ocean by a factor of 2.34 This surge was further fueled by ongoing new anthropogenic Hg emissions and marine Hg deposition. This suppressed response in surface ocean Hg likely explains the absence of significant decreasing trends in tuna Hg levels following the decrease in emissions in the 1970s. Subsurface ocean legacy Hg is likely to buffer Hg mass in the surface ocean for decades, partly depending on future emission scenarios (Figure 3). Under the maximum feasible reduction scenario, while the Hg mass in the atmosphere is expected to decrease immediately, Hg masses in the surface and subsurface oceans are predicted to take 10 and 25 years, respectively, to start decreasing. Under the new policy scenario, these response delays are expected to extend to 25 and 45 years, respectively. Inhabiting the surface (mainly skipjack and yellowfin) and subsurface (bigeye) waters, tropical tunas likely reflect this time lag between the atmosphere and the different ocean layers. Tuna Hg concentrations may therefore take several decades to decrease as a result of the emission reduction measures.

The box model also illustrates how the surface ocean responds more quickly to an increase in emissions and deposition than to a decrease. The 5-fold increase in Hg emissions in the 19th century led to immediate 4- and 3-fold increases in surface and subsurface ocean Hg by 1900, respectively, yet the 5-fold decrease in Hg emissions by 2050 under the maximum feasible reduction scenario induces an only 7% decrease in surface ocean Hg and even a 10% increase in subsurface ocean Hg. This explains why tuna Hg concentrations in the northwestern Pacific have reacted rapidly to the recent increase in Asian Hg emissions and releases.

Possible ecological and biogeochemical confounding processes

As the Hg box model lacks spatial resolution and does not include aquatic food webs, it precludes the investigation of local and regional impacts resulting from marine biogeochemical and tuna ecological processes. However, these processes play a pivotal role in governing the net production, bioavailability, and biomagnification of MeHg.

Since the 1970s, the oceanic environment has experienced anthropogenically forced warming of the upper ocean.⁵⁶ Seawater warming, leading to a shift in foraging habitat toward higher latitudes or deeper in the water column, is anticipated to increase MeHg concentrations in marine top predators.³⁸ However, tropical tunas were shown to display relative site fidelity globally from the 1970s to 2010s.²⁴ Moreover, yellowfin and bigeye trophic positions were shown to remain stable between 2001 and 2015 globally.⁵⁷ Our re-evaluation of tuna $\delta^{15}\text{N}$ values with new data in the southwestern Pacific, western Indian, and eastern central Atlantic confirms stable trophic positions for the three tropical tunas over time (2001–2022), suggesting no changes in tuna foraging depth or diet that could have biased the tuna Hg time series in these three regions (Figure S4 and Table S5). For skipjack in the northwestern Pacific, long-term trophic time series would, however, be necessary to fully exclude any trophic bias. Changes in ocean productivity and nutrient enrichment of coastal ecosystems may also

have confounding effects on decadal trends of tuna Hg, as primary production and carbon export are key drivers of MeHg at depth.^{58,59} However, the spatial gradients in these properties are far greater than long-term temporal trends, and the signal of secular changes may be engulfed by the noise of inter-annual variability in these properties (Figure S5). Taken together, this suggests stable long-term trends in the net production of MeHg but high inter-annual variability, which may in turn explain the strong year-to-year variability in tuna Hg.

In the coming decades, climate-induced changes in ocean biogeochemistry are expected to induce substantial regional variabilities in MeHg formation and bioaccumulation at the base of marine food webs,⁶⁰ potentially affecting tuna Hg levels. At present, our understanding of these regional changes is insufficient to quantify their interference with changes in Hg emissions and cycling in the environment. Consequently, extended time series of Hg concentrations and speciation in seawater, phytoplankton, and zooplankton are urgently needed to explore how climate-driven regional processes might offset or enhance measures aimed at reducing emissions.

Implications for mercury monitoring in the global ocean

With the adoption of the Minamata Convention, Hg biomonitoring in seafood is needed to evaluate the effectiveness of political decisions and reduction efforts in relation to human health.⁶¹ With the exception of the northwestern Pacific, we show stable long-term Hg concentrations in tunas but year-to-year variability, which likely reflects natural biogeochemical and/or ecological processes. Conversely, skipjack Hg concentrations near Asia increased significantly in the late 1990s, reaching concentrations up to 4 times higher than those elsewhere in the global ocean. These temporal trends suggest that at the local scale along Asian coasts close to large Hg emissions hot spots, Hg concentrations in surface tuna may integrate the increased level of deposition from nearby anthropogenic Hg release over time; yet on a global scale, the divergence between stable tuna Hg concentrations and global variations in the emission and deposition of Hg likely reflects the inertia of subsurface ocean legacy Hg that continues to supply subsurface and surface ocean food webs. Taken together, our results show that Hg concentrations in tropical tunas can reflect concomitant increasing anthropogenic emissions of Hg to the atmosphere, but may take decades to decrease following emission reduction measures. We estimate that only the maximum feasible reduction policy scenario would lead to a detectable decrease in surface ocean tuna Hg levels and achieve the objective of the Minamata Convention in the near future.

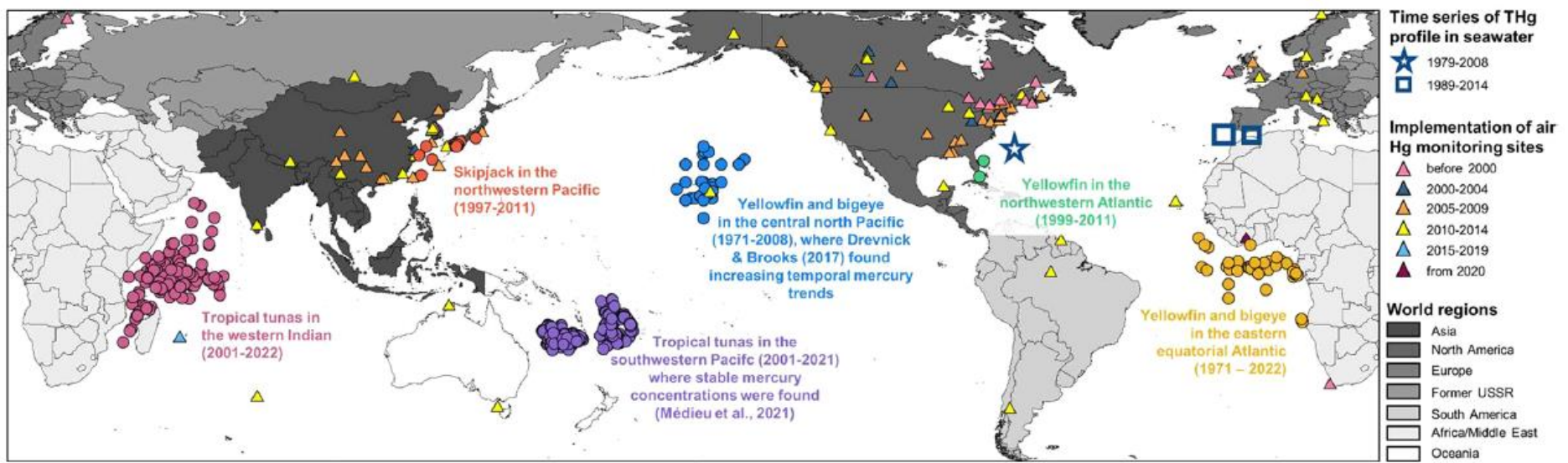


Figure 1. Origin of the tropical tuna samples. The temporal variability of mercury (Hg) concentrations was investigated in tropical tuna samples in six regions of the global ocean. Colored dots represent tuna catch locations, while colored triangles show air monitoring sites according to their starting year. The blue star and squares represent the three locations where seawater concentration profiles of total mercury (THg) are available in multiple years.^{16,17} Countries are colored following the definition of the seven world regions in the emission inventory of Streets et al.^{10,11,29,30}

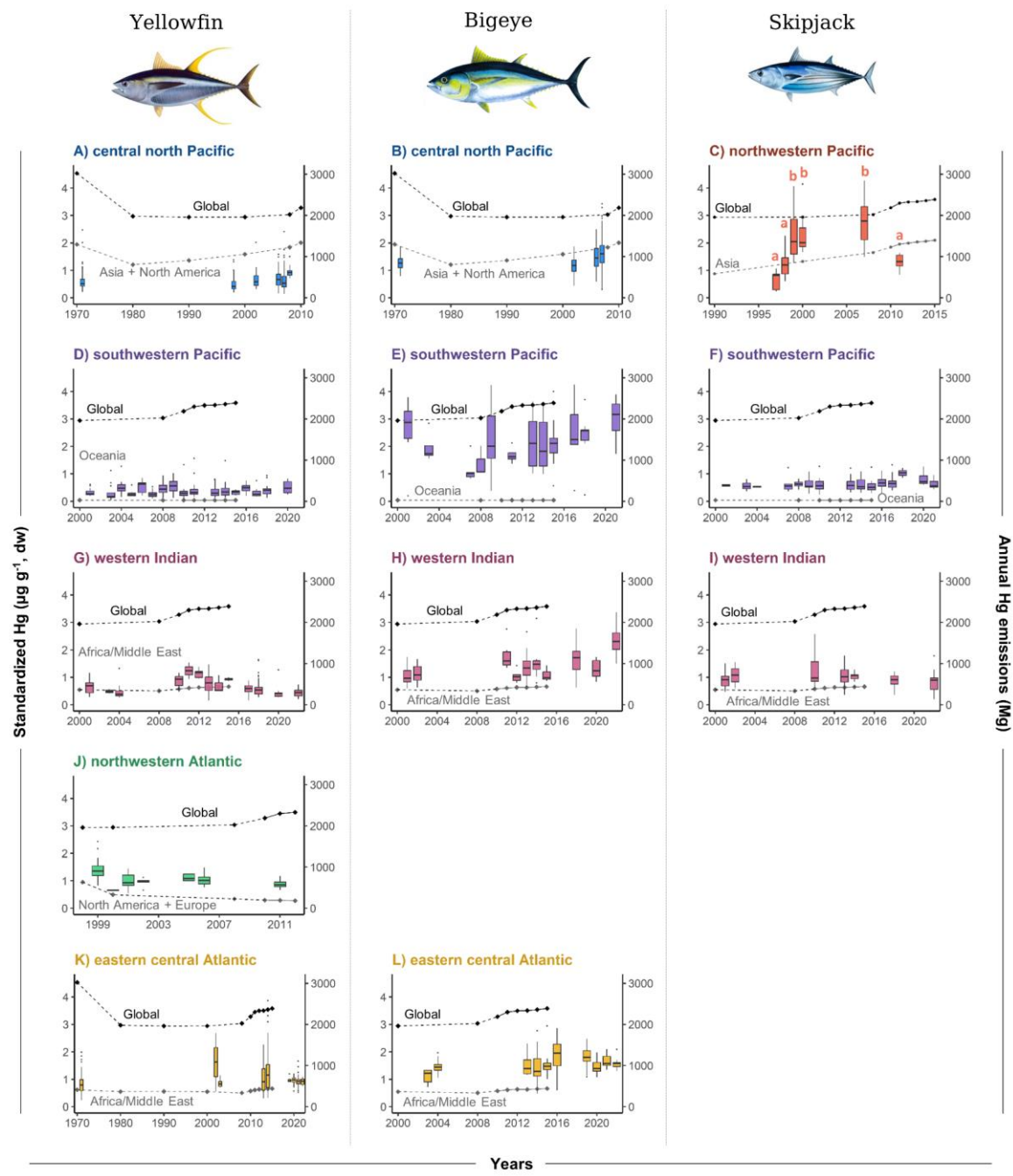


Figure 2. Temporal variability of tuna mercury concentrations and anthropogenic emissions. Box plots of standardized mercury (Hg) concentrations (micrograms per gram, dw) vs time in (A) yellowfin and (B) bigeye in the central north Pacific (1971–2008), (C) skipjack in the northwestern Pacific (1997–2011), (D) yellowfin, (E) bigeye, and (F) skipjack in the southwestern Pacific (2001–2021), (G) yellowfin, (H) bigeye, and (I) skipjack in the western Indian (2001–2022), (J) yellowfin in the northwestern Atlantic (1999–2011), and (K) yellowfin and (L) bigeye in the eastern central Atlantic (1971–2022). A significant increase was found in the skipjack standardized Hg content in the northwestern Pacific only, as symbolized by the letters in panel C. Elsewhere, the year-to-year comparison indicates a nonsignificant difference between old and recent Hg data. Diamonds represent mean regional (dark gray) and global (black) anthropogenic Hg emissions (Mg) to the atmosphere estimated by the emission inventory of Streets et al.^{10,11,29,30} Solid lines show annual trends of emissions for the period of 2010–2015, while dashed lines show decadal trends of emissions for the period of 1970–2010. Note that the x-axes (sampling years) are adjusted to each time series for the sake of clarity. Tuna illustrations were created by Les Hata, @SPC.

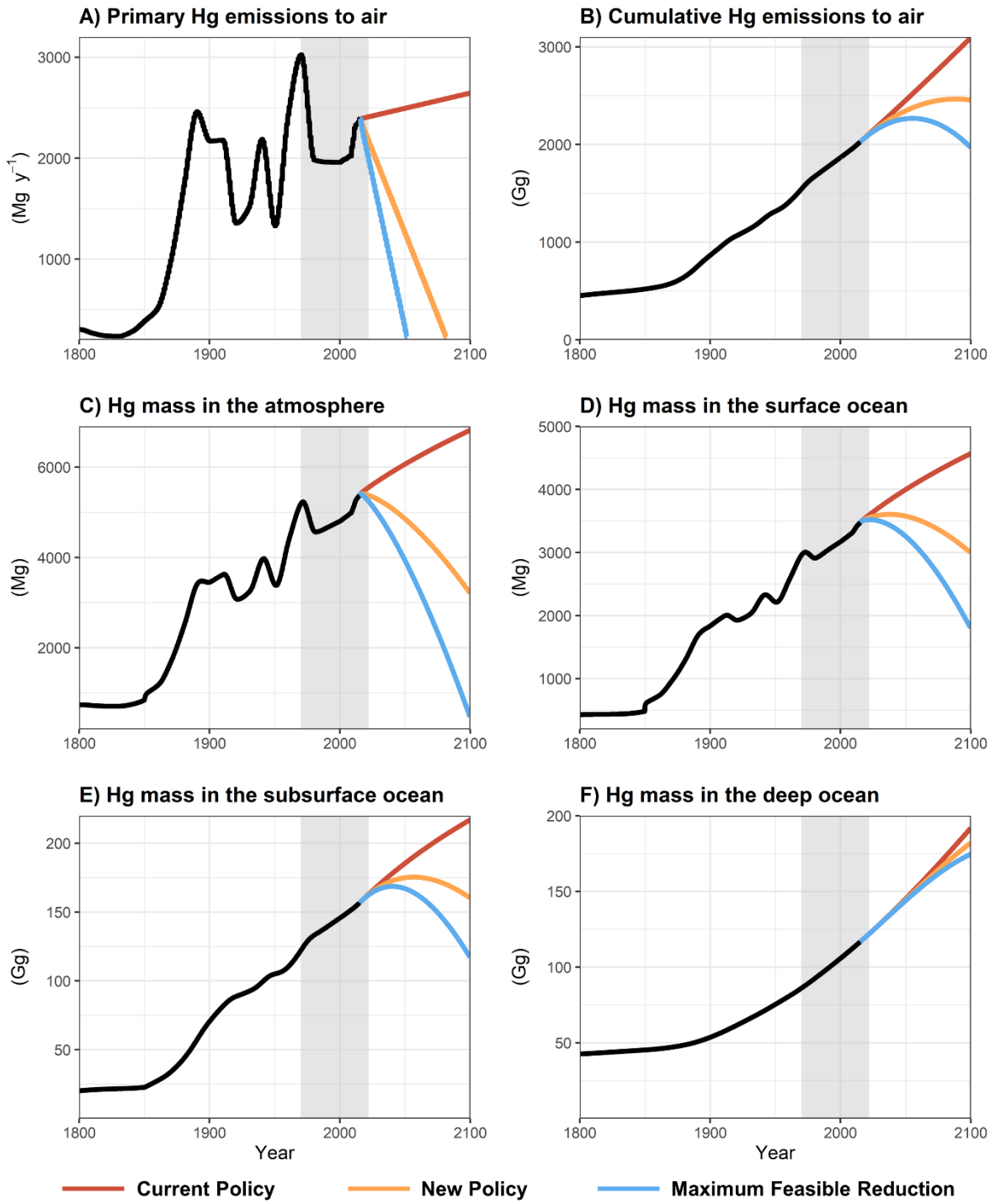


Figure 3. Simulated global anthropogenic influence on environmental mercury (Hg) loads using the box model of Amos et al.,^{33,34} the emission inventory of Streets et al.^{10,11,29,30} up to 2015, and three emissions scenarios for the period of 2016–2100: current policy (red), new policy (orange), and maximum feasible reduction (blue), as defined by Angot et al.³⁵ and Pacyna et al.³⁶ (A and B) Annual (megagrams per year) and cumulative (gigagrams) primary anthropogenic Hg emissions to air, respectively. (C–F) Temporal evolution of Hg masses (Mg or Gg) in the atmosphere and the surface (extended to the base of the mixed layer, ~50 m), subsurface (extending to the depth of the permanent thermocline, ~1500 m), and deep (extending to the sea floors) oceans, respectively. The gray bands indicate our study period (1971–2022).

Acknowledgements:

This study was conducted in the framework of ANR-17-CE34-0010 MERTOX (unraveling the origin of methylmercury toxin in marine ecosystems, PI David Point) from the French Agence Nationale de la Recherche and was assisted by collaborations under the international framework of the IMBeR regional program Climate Impacts On Oceanic Top Predators (CLIO TOP). This study also benefited from financial support from the Région Bretagne and Université de Bretagne Occidentale (UBO). The authors thank all of the fishermen, observers, port samplers, and technical staff who participated in the collection and preparation of tuna samples. In the Atlantic and Indian oceans, the authors are grateful to the UAR IMAGO of IRD and the volunteers involved in the French PIRATA cruises (10.18142/14) and to the SFA-IRD and CRO-IRD-IEO teams. In the Pacific Ocean, the authors thank the WCPFC Tuna Tissue Bank, the Pacific Marine Specimen Bank managed by the Pacific Community (SPC), the Environmental Specimen Bank of Ehime University, and the NOAA Pacific Islands Region Observer Program. The authors are grateful to Emmanuel Chassot from IOTC (Seychelles) for providing species-specific length-weight relationships. AM thanks L'Institut Agro Rennes-Angers for its hospitality. PB is an honorary member of the IUF (Institut Universitaire de France). This study benefited from thoughtful comments from three anonymous referees.

References

- (1) Outridge, P. M.; Mason, R. P.; Wang, F.; Guerrero, S.; Heimbürger-Boavida, L. E. Updated Global and Oceanic Mercury Budgets for the United Nations Global Mercury Assessment 2018. *Environ. Sci. Technol.* **2018**, 52 (20), 11466–11477. <https://doi.org/10.1021/acs.est.8b01246>.
- (2) Villar, E.; Cabrol, L.; Heimbürger-Boavida, L.-E. Widespread Microbial Mercury Methylation Genes in the Global Ocean. *Environmental Microbiology Reports* **2020**, 12 (3), 277–287. <https://doi.org/10.1111/1758-2229.12829>.
- (3) Axelrad, D. A.; Bellinger, D. C.; Ryan, L. M.; Woodruff, T. J. Dose–Response Relationship of Prenatal Mercury Exposure and IQ: An Integrative Analysis of Epidemiologic Data. *Environmental Health Perspectives* **2007**, 115 (4), 609–615. <https://doi.org/10.1289/ehp.9303>.
- (4) Genchi, G.; Sinicropi, M.; Carocci, A.; Lauria, G.; Catalano, A. Mercury Exposure and Heart Diseases. *IJERPH* **2017**, 14 (1), 74. <https://doi.org/10.3390/ijerph14010074>.
- (5) *The State of World Fisheries and Aquaculture 2018 - Meeting the Sustainable Development Goals*; FAO, Ed.; Rome, 2018.
- (6) Bodin, N.; Lesperance, D.; Albert, R.; Hollanda, S.; Michaud, P.; Degroote, M.; Churlaud, C.; Bustamante, P. Trace Elements in Oceanic Pelagic Communities in the Western Indian Ocean. *Chemosphere* **2017**, 174, 354–362. <https://doi.org/10.1016/j.chemosphere.2017.01.099>.
- (7) Choy, C. A.; Popp, B. N.; Kaneko, J. J.; Drazen, J. C. The Influence of Depth on Mercury Levels in Pelagic Fishes and Their Prey. *Proceedings of the National Academy of Sciences* **2009**, 106 (33), 13865–13869. <https://doi.org/10.1073/pnas.0900711106>.
- (8) Houssard, P.; Point, D.; Tremblay-Boyer, L.; Allain, V.; Pethybridge, H.; Masbou, J.; Ferriss, B. E.; Baya, P. A.; Lagane, C.; Menkes, C. E.; Letourneau, Y.; Lorrain, A. A Model of Mercury Distribution in Tuna from the Western and Central Pacific Ocean: Influence of Physiology, Ecology and Environmental Factors. *Environmental Science & Technology* **2019**, 53 (3), 1422–1431. <https://doi.org/10.1021/acs.est.8b06058>.
- (9) Zhang, Y.; Song, Z.; Huang, S.; Zhang, P.; Peng, Y.; Wu, P.; Gu, J.; Dutkiewicz, S.; Zhang, H.; Wu, S.; Wang, F.; Chen, L.; Wang, S.; Li, P. Global Health Effects of Future Atmospheric Mercury Emissions. *Nat Commun* **2021**, 12 (1), 3035. <https://doi.org/10.1038/s41467-021-23391-7>.
- (10) Streets, D. G.; Horowitz, H. M.; Lu, Z.; Levin, L.; Thackray, C. P.; Sunderland, E. M. Five Hundred Years of Anthropogenic Mercury: Spatial and Temporal Release Profiles. *Environ. Res. Lett.* **2019**, 14 (8), 084004. <https://doi.org/10.1088/1748-9326/ab281f>.
- (11) Streets, D. G.; Horowitz, H. M.; Lu, Z.; Levin, L.; Thackray, C. P.; Sunderland, E. M. Global and Regional Trends in Mercury Emissions and Concentrations, 2010–2015. *Atmospheric Environment* **2019**, 201, 417–427. <https://doi.org/10.1016/j.atmosenv.2018.12.031>.
- (12) Selin, N. E.; Jacob, D. J.; Yantosca, R. M.; Strode, S.; Jaeglé, L.; Sunderland, E. M. Global 3-D Land-Ocean-Atmosphere Model for Mercury: Present-Day versus Preindustrial Cycles and Anthropogenic Enrichment Factors for Deposition. *Global Biogeochemical Cycles* **2008**, 22 (2), 13. <https://doi.org/10.1029/2007GB003040>.
- (13) Sonke, J. E.; Angot, H.; Zhang, Y.; Poulain, A.; Björn, E.; Schartup, A. Global Change Effects on Biogeochemical Mercury Cycling. *Ambio* **2023**, 52 (5), 853–876. <https://doi.org/10.1007/s13280-023-01855-y>.
- (14) Sprovieri, F.; Pirrone, N.; Bencardino, M.; D’Amore, F.; Carbone, F.; Cinnirella, S.; Mannarino, V.; Landis, M.; Ebinghaus, R.; Weigelt, A.; Brunke, E.-G.; Labuschagne, C.; Martin, L.; Munthe, J.; Wängberg, I.; Artaxo, P.; Morais, F.; Barbosa, H. de M. J.; Brito, J.; Cairns, W.; Barbante, C.; Diéguez, M. del C.; Garcia, P. E.; Dommergue, A.; Angot, H.; Magand, O.; Skov, H.; Horvat, M.; Kotnik, J.; Read, K. A.; Neves, L. M.; Gawlik, B. M.; Sena, F.; Mashyanov, N.; Obolkin, V.; Wip, D.; Feng, X. B.; Zhang, H.; Fu, X.; Ramachandran, R.; Cossa, D.; Knoery, J.; Maruscak, N.; Nerentorp, M.; Norstrom, C. Atmospheric Mercury Concentrations Observed at Ground-Based Monitoring

- Sites Globally Distributed in the Framework of the GMOS Network. *Atmospheric Chemistry and Physics* **2016**, *16* (18), 11915–11935. <https://doi.org/10.5194/acp-16-11915-2016>.
- (15) Lamborg, C. H.; Hammerschmidt, C. R.; Bowman, K. L.; Swarr, G. J.; Munson, K. M.; Ohnemus, D. C.; Lam, P. J.; Heimbürger, L.-E.; Rijkenberg, M. J. A.; Saito, M. A. A Global Ocean Inventory of Anthropogenic Mercury Based on Water Column Measurements. *Nature* **2014**, *512* (7512), 65–68. <https://doi.org/10.1038/nature13563>.
- (16) Mason, R. P.; Choi, A. L.; Fitzgerald, W. F.; Hammerschmidt, C. R.; Lamborg, C. H.; Soerensen, A. L.; Sunderland, E. M. Mercury Biogeochemical Cycling in the Ocean and Policy Implications. *Environmental Research* **2012**, *119*, 101–117. <https://doi.org/10.1016/j.envres.2012.03.013>.
- (17) Cossa, D.; Knoery, J.; Boye, M.; Maruszak, N.; Thomas, B.; Courau, P.; Sprovieri, F. Oceanic Mercury Concentrations on Both Sides of the Strait of Gibraltar Decreased between 1989 and 2012. *Anthropocene* **2020**, *29*, 100230. <https://doi.org/10.1016/j.ancene.2019.100230>.
- (18) Drevnick, P. E.; Lamborg, C. H.; Horgan, M. J. Increase in Mercury in Pacific Yellowfin Tuna: Mercury in Yellowfin Tuna. *Environ Toxicol Chem* **2015**, *34* (4), 931–934. <https://doi.org/10.1002/etc.2883>.
- (19) Drevnick, P. E.; Brooks, B. A. Mercury in Tunas and Blue Marlin in the North Pacific Ocean. *Environmental Toxicology and Chemistry* **2017**, *36* (5), 1365–1374. <https://doi.org/10.1002/etc.3757>.
- (20) Lee, C.-S.; Lutcavage, M. E.; Chandler, E.; Madigan, D. J.; Cerrato, R. M.; Fisher, N. S. Declining Mercury Concentrations in Bluefin Tuna Reflect Reduced Emissions to the North Atlantic Ocean. *Environmental Science & Technology* **2016**, *50* (23), 12825–12830. <https://doi.org/10.1021/acs.est.6b04328>.
- (21) Médieu, A.; Point, D.; Receveur, A.; Gauthier, O.; Allain, V.; Pethybridge, H.; Menkes, C. E.; Gillikin, D. P.; Revill, A. T.; Somes, C. J.; Collin, J.; Lorrain, A. Stable Mercury Concentrations of Tropical Tuna in the South Western Pacific Ocean: An 18-Year Monitoring Study. *Chemosphere* **2021**, *263*, 128024. <https://doi.org/10.1016/j.chemosphere.2020.128024>.
- (22) Olson, R. J.; Young, J. W.; Ménard, F.; Potier, M.; Allain, V.; Goñi, N.; Logan, J. M.; Galván-Magaña, F. Chapter Four: Bioenergetics, Trophic Ecology, and Niche Separation of Tunas. In *Advances in Marine Biology*; Elsevier, 2016; Vol. 74, pp 199–344. <https://doi.org/10.1016/bs.amb.2016.06.002>.
- (23) Murua, H.; Rodriguez-Marin, E.; Neilson, J. D.; Farley, J. H.; Juan-Jordá, M. J. Fast versus Slow Growing Tuna Species: Age, Growth, and Implications for Population Dynamics and Fisheries Management. *Rev Fish Biol Fisheries* **2017**, *27* (4), 733–773. <https://doi.org/10.1007/s11160-017-9474-1>.
- (24) Fonteneau, A.; Hallier, J.-P. Fifty Years of Dart Tag Recoveries for Tropical Tuna: A Global Comparison of Results for the Western Pacific, Eastern Pacific, Atlantic, and Indian Oceans. *Fisheries Research* **2015**, *163*, 7–22. <https://doi.org/10.1016/j.fishres.2014.03.022>.
- (25) Houssard, P.; Lorrain, A.; Tremblay-Boyer, L.; Allain, V.; Graham, B. S.; Menkes, C. E.; Pethybridge, H.; Couturier, L. I. E.; Point, D.; Leroy, B.; Receveur, A.; Hunt, B. P. V.; Vourey, E.; Bonnet, S.; Rodier, M.; Raimbault, P.; Feunteun, E.; Kuhnert, P. M.; Munaron, J.-M.; Lebreton, B.; Otake, T.; Letourneau, Y. Trophic Position Increases with Thermocline Depth in Yellowfin and Bigeye Tuna across the Western and Central Pacific Ocean. *Progress in Oceanography* **2017**, *154*, 49–63. <https://doi.org/10.1016/j.pocean.2017.04.008>.
- (26) Block, B. A.; Teo, S. L. H.; Walli, A.; Boustany, A.; Stokesbury, M. J. W.; Farwell, C. J.; Weng, K. C.; Dewar, H.; Williams, T. D. Electronic Tagging and Population Structure of Atlantic Bluefin Tuna. *Nature* **2005**, *434* (7037), 1121–1127. <https://doi.org/10.1038/nature03463>.
- (27) Hobday, A.; Evans, K.; Eveson, J. P.; Farley, J.; Hartog, J.; Basson, M.; Patterson, T. Distribution and Migration—Southern Bluefin Tuna (*Thunnus Maccoyii*). In *Biology and Ecology of Bluefin Tuna*; 2015; pp 189–210. <https://doi.org/10.1201/b18714-12>.

- (28) Madigan, D. J.; Baumann, Z.; Carlisle, A. B.; Hoen, D. K.; Popp, B. N.; Dewar, H.; Snodgrass, O. E.; Block, B. A.; Fisher, N. S. Reconstructing Transoceanic Migration Patterns of Pacific Bluefin Tuna Using a Chemical Tracer Toolbox. *Ecology* **2014**, *95* (6), 1674–1683. <https://doi.org/10.1890/13-1467.1>.
- (29) Streets, D. G.; Horowitz, H. M.; Jacob, D. J.; Lu, Z.; Levin, L.; ter Schure, A. F. H.; Sunderland, E. M. Total Mercury Released to the Environment by Human Activities. *Environ. Sci. Technol.* **2017**, *51* (11), 5969–5977. <https://doi.org/10.1021/acs.est.7b00451>.
- (30) Streets, D. G.; Devane, M. K.; Lu, Z.; Bond, T. C.; Sunderland, E. M.; Jacob, D. J. All-Time Releases of Mercury to the Atmosphere from Human Activities. *Environmental Science & Technology* **2011**, *45* (24), 10485–10491. <https://doi.org/10.1021/es202765m>.
- (31) Médieu, A.; Lorrain, A.; Point, D. Are Tunas Relevant Bioindicators of Mercury Concentrations in the Global Ocean? *Ecotoxicology* **2023**. <https://doi.org/10.1007/s10646-023-02679-y>.
- (32) Médieu, A.; Point, D.; Itai, T.; Angot, H.; Buchanan, P. J.; Allain, V.; Fuller, L.; Griffiths, S.; Gillikin, D. P.; Sonke, J. E.; Heimbürger-Boavida, L.-E.; Desgranges, M.-M.; Menkes, C. E.; Madigan, D. J.; Brosset, P.; Gauthier, O.; Tagliabue, A.; Bopp, L.; Verheyden, A.; Lorrain, A. Evidence That Pacific Tuna Mercury Levels Are Driven by Marine Methylmercury Production and Anthropogenic Inputs. *PNAS* **2022**, *119* (2), 8. <https://doi.org/10.1073/pnas.2113032119>.
- (33) Amos, H. M.; Sonke, J. E.; Obrist, D.; Robins, N.; Hagan, N.; Horowitz, H. M.; Mason, R. P.; Witt, M.; Hedgecock, I. M.; Corbitt, E. S.; Sunderland, E. M. Observational and Modeling Constraints on Global Anthropogenic Enrichment of Mercury. *Environ. Sci. Technol.* **2015**, *49* (7), 4036–4047. <https://doi.org/10.1021/es5058665>.
- (34) Amos, H. M.; Jacob, D. J.; Streets, D. G.; Sunderland, E. M. Legacy Impacts of All-Time Anthropogenic Emissions on the Global Mercury Cycle. *Global Biogeochemical Cycles* **2013**, *27* (2), 410–421. <https://doi.org/10.1002/gbc.20040>.
- (35) Angot, H.; Hoffman, N.; Giang, A.; Thackray, C. P.; Hendricks, A. N.; Urban, N. R.; Selin, N. E. Global and Local Impacts of Delayed Mercury Mitigation Efforts. *Environ. Sci. Technol.* **2018**, *52* (22), 12968–12977. <https://doi.org/10.1021/acs.est.8b04542>.
- (36) Pacyna, J. M.; Travnikov, O.; De Simone, F.; Hedgecock, I. M.; Sundseth, K.; Pacyna, E. G.; Steenhuisen, F.; Pirrone, N.; Munthe, J.; Kindbom, K. Current and Future Levels of Mercury Atmospheric Pollution on a Global Scale. *Atmospheric Chemistry and Physics* **2016**, *16* (19), 12495–12511. <https://doi.org/10.5194/acp-16-12495-2016>.
- (37) Kraepiel, A. M. L.; Keller, K.; Chin, H. B.; Malcolm, E. G.; Morel, F. M. M. Sources and Variations of Mercury in Tuna. *Environ. Sci. Technol.* **2003**, *37* (24), 5551–5558.
- (38) Schartup, A. T.; Thackray, C. P.; Qureshi, A.; Dassuncao, C.; Gillespie, K.; Hanke, A.; Sunderland, E. M. Climate Change and Overfishing Increase Neurotoxicant in Marine Predators. *Nature* **2019**, *572*, 648–650.
- (39) Barbosa, R. V.; Point, D.; Médieu, A.; Allain, V.; Gillikin, D. P.; Couturier, L. I. E.; Munaron, J.-M.; Roupsard, F.; Lorrain, A. Mercury Concentrations in Tuna Blood and Muscle Mirror Seawater Methylmercury in the Western and Central Pacific Ocean. *Marine Pollution Bulletin* **2022**, *180*, 113801. <https://doi.org/10.1016/j.marpolbul.2022.113801>.
- (40) *Atmospheric Mercury Network, AMNet*. <https://nadp.slh.wisc.edu/networks/atmospheric-mercury-network/> (accessed 2023-05-30).
- (41) *European Monitoring and Evaluation Program, EMEP*. <https://www.emep.int/> (accessed 2023-05-30).
- (42) UN Environment. *Global Mercury Assessment 2018*; UN Environment Programme Chemicals and Health Branch Geneva Switzerland, 2019.
- (43) Li, C.; Sonke, J. E.; Le Roux, G.; Piotrowska, N.; Van der Putten, N.; Roberts, S. J.; Daley, T.; Rice, E.; Gehrels, R.; Enrico, M.; Mauquoy, D.; Roland, T. P.; De Vleeschouwer, F. Unequal Anthropogenic Enrichment of Mercury in Earth's Northern and Southern Hemispheres. *ACS*

- Earth Space Chem.* **2020**, *4* (11), 2073–2081.
<https://doi.org/10.1021/acsearthspacechem.0c00220>.
- (44) Laurier, F. J. G.; Mason, R. P.; Gill, G. A.; Whalin, L. Mercury Distributions in the North Pacific Ocean—20 Years of Observations. *Marine Chemistry* **2004**, *90* (1), 3–19.
<https://doi.org/10.1016/j.marchem.2004.02.025>.
- (45) Fu, X.; Feng, X.; Zhang, G.; Xu, W.; Li, X.; Yao, H.; Liang, P.; Li, J.; Sommar, J.; Yin, R.; Liu, N. Mercury in the Marine Boundary Layer and Seawater of the South China Sea: Concentrations, Sea/Air Flux, and Implication for Land Outflow. *J. Geophys. Res.* **2010**, *115* (D6), D06303.
<https://doi.org/10.1029/2009JD012958>.
- (46) Kim, H.; Lee, K.; Lim, D.-I.; Nam, S.-I.; Han, S. hee; Kim, J.; Lee, E.; Han, I.-S.; Jin, Y. K.; Zhang, Y. Increase in Anthropogenic Mercury in Marginal Sea Sediments of the Northwest Pacific Ocean. *Science of The Total Environment* **2019**, *654*, 801–810.
<https://doi.org/10.1016/j.scitotenv.2018.11.076>.
- (47) Tseng, C.-M.; Ang, S.-J.; Chen, Y.-S.; Shiao, J.-C.; Lamborg, C. H.; He, X.; Reinfelder, J. R. Bluefin Tuna Reveal Global Patterns of Mercury Pollution and Bioavailability in the World's Oceans. *Proceedings of the National Academy of Sciences* **2021**, *118* (38), e2111205118.
<https://doi.org/10.1073/pnas.2111205118>.
- (48) Marumoto, K.; Suzuki, N.; Shibata, Y.; Takeuchi, A.; Takami, A.; Fukuzaki, N.; Kawamoto, K.; Mizohata, A.; Kato, S.; Yamamoto, T.; Chen, J.; Hattori, T.; Nagasaka, H.; Saito, M. Long-Term Observation of Atmospheric Speciated Mercury during 2007–2018 at Cape Hedo, Okinawa, Japan. *Atmosphere* **2019**, *10* (7), 362. <https://doi.org/10.3390/atmos10070362>.
- (49) Nguyen, L. S. P.; Sheu, G.-R.; Lin, D.-W.; Lin, N.-H. Temporal Changes in Atmospheric Mercury Concentrations at a Background Mountain Site Downwind of the East Asia Continent in 2006–2016. *Science of The Total Environment* **2019**, *686*, 1049–1056.
<https://doi.org/10.1016/j.scitotenv.2019.05.425>.
- (50) Shi, J.; Chen, Y.; Xu, L.; Hong, Y.; Li, M.; Fan, X.; Yin, L.; Chen, Y.; Yang, C.; Chen, G.; Liu, T.; Ji, X.; Chen, J. Measurement Report: Atmospheric Mercury in a Coastal City of Southeast China – Inter-Annual Variations and Influencing Factors. *Atmospheric Chemistry and Physics* **2022**, *22* (17), 11187–11202. <https://doi.org/10.5194/acp-22-11187-2022>.
- (51) Tang, Y.; Wang, S.; Wu, Q.; Liu, K.; Wang, L.; Li, S.; Gao, W.; Zhang, L.; Zheng, H.; Li, Z.; Hao, J. Recent Decrease Trend of Atmospheric Mercury Concentrations in East China: The Influence of Anthropogenic Emissions. *Atmospheric Chemistry and Physics* **2018**, *18* (11), 8279–8291.
<https://doi.org/10.5194/acp-18-8279-2018>.
- (52) Zhang, Y.; Zhang, L.; Cao, S.; Liu, X.; Jin, J.; Zhao, Y. Improved Anthropogenic Mercury Emission Inventories for China from 1980 to 2020: Toward More Accurate Effectiveness Evaluation for the Minamata Convention. *Environ. Sci. Technol.* **2023**, *57* (23), 8660–8670.
<https://doi.org/10.1021/acs.est.3c01065>.
- (53) Zheng, B.; Tong, D.; Li, M.; Liu, F.; Hong, C.; Geng, G.; Li, H.; Li, X.; Peng, L.; Qi, J.; Yan, L.; Zhang, Y.; Zhao, H.; Zheng, Y.; He, K.; Zhang, Q. Trends in China's Anthropogenic Emissions since 2010 as the Consequence of Clean Air Actions. *Atmospheric Chemistry and Physics* **2018**, *18* (19), 14095–14111. <https://doi.org/10.5194/acp-18-14095-2018>.
- (54) Wang, F.; Outridge, P. M.; Feng, X.; Meng, B.; Heimbürger-Boavida, L.-E.; Mason, R. P. How Closely Do Mercury Trends in Fish and Other Aquatic Wildlife Track Those in the Atmosphere? - Implications for Evaluating the Effectiveness of the Minamata Convention. *Science of the Total Environment* **2019**, *674*, 58–70. <https://doi.org/10.1016/j.scitotenv.2019.04.101>.
- (55) Zhang, Y.; Zhang, P.; Song, Z.; Huang, S.; Yuan, T.; Wu, P.; Shah, V.; Liu, M.; Chen, L.; Wang, X.; Zhou, J.; Agnan, Y. An Updated Global Mercury Budget from a Coupled Atmosphere-Land-Ocean Model: 40% More Re-Emissions Buffer the Effect of Primary Emission Reductions. *One Earth* **2023**, *6* (3), 316–325. <https://doi.org/10.1016/j.oneear.2023.02.004>.

- (56) Bindoff, N. L.; Cheung, W. W. L.; Kairo, J. G.; Arístegui, J.; Guinder, V. A.; Hallberg, R.; Hilmi, N. J. M.; Jiao, N.; Karim, M. S.; Levin, L.; O'Donoghue, S.; Purca Cuicapusa, S. R.; Rinkevich, B.; Suga, T.; Tagliabue, A.; Williamson, P. Changing Ocean, Marine Ecosystems, and Dependent Communities. In *IPCC Special Report on the Ocean and Cryosphere in a Changing Climate*; Pörtner, H.-O., Roberts, D. C., Masson-Delmotte, V., Zhai, P., Tignor, M., Poloczanska, E., Mintenbeck, K., Alegría, A., Nicolai, M., Okem, A., Petzold, J., Rama, B., Weyer, N. M., Eds.; Intergovernmental Panel on Climate Change: Switzerland, 2019; pp 477–587.
- (57) Lorrain, A.; Pethybridge, H.; Cassar, N.; Receveur, A.; Allain, V.; Bodin, N.; Bopp, L.; Choy, C. A.; Duffy, L.; Fry, B.; Goñi, N.; Graham, B. S.; Hobday, A. J.; Logan, J. M.; Ménard, F.; Menkes, C. E.; Olson, R. J.; Pagendam, D. E.; Point, D.; Revill, A. T.; Somes, C. J.; Young, J. W. Trends in Tuna Carbon Isotopes Suggest Global Changes in Pelagic Phytoplankton Communities. *Glob Change Biol* **2020**, 26 (2), 458–470. <https://doi.org/10.1111/gcb.14858>.
- (58) Heimbürger, L.-E.; Cossa, D.; Marty, J.-C.; Migon, C.; Averyt, B.; Dufour, A.; Ras, J. Methyl Mercury Distributions in Relation to the Presence of Nano- and Picophytoplankton in an Oceanic Water Column (Ligurian Sea, North-Western Mediterranean). *Geochimica et Cosmochimica Acta* **2010**, 74 (19), 5549–5559. <https://doi.org/10.1016/j.gca.2010.06.036>.
- (59) Sunderland, E. M.; Krabbenhoft, D. P.; Moreau, J. W.; Strode, S. A.; Landing, W. M. Mercury Sources, Distribution, and Bioavailability in the North Pacific Ocean: Insights from Data and Models. *Global Biogeochemical Cycles* **2009**, 23 (2), 14. <https://doi.org/10.1029/2008GB003425>.
- (60) Zhang, Y.; Dutkiewicz, S.; Sunderland, E. M. Impacts of Climate Change on Methylmercury Formation and Bioaccumulation in the 21st Century Ocean. *One Earth* **2021**, 4 (2), 279–288. <https://doi.org/10.1016/j.oneear.2021.01.005>.
- (61) Evers, D. C.; Keane, S. E.; Basu, N.; Buck, D. Evaluating the Effectiveness of the Minamata Convention on Mercury: Principles and Recommendations for next Steps. *Science of The Total Environment* **2016**, 569–570, 888–903. <https://doi.org/10.1016/j.scitotenv.2016.05.001>.

Supplementary Information for

Stable tuna mercury concentrations since 1971 illustrate marine inertia and the need for strong emission reductions under the Minamata Convention

Anaïs Médieu, David Point, Jeroen E. Sonke, Hélène Angot, Valérie Allain, Nathalie Bodin, Douglas H. Adams, Anders Bignert, David G. Streets, Pearse B. Buchanan, Lars-Eric Heimbürger-Boavida, Heidi Pethybridge, David P. Gillikin, Frédéric Ménard, C. Anela Choy, Takaaki Itai, Paco Bustamante, Zahrah Dhurmeea, Bridget E. Ferriss, Bernard Bourlès, Jérémie Habasque, Anouk Verheyden, Jean-Marie Munaron, Laure Laffont, Olivier Gauthier, Anne Lorrain

This PDF file includes:

Material and methods supplementary information

Figures S1 to S5

Tables S1 to S4

Supplementary information on material and methods

Tuna sampling and data compilation: We assembled 2,910 (i.e., 1,852 published and 1,058 unpublished) tuna muscle Hg concentrations in six regions of the Pacific, Atlantic and Indian Oceans, allowing temporal analysis covering approximately 50 years from 1971 to 2022, depending on the regions. In the Pacific Ocean, this corresponds to 512 yellowfin (1971-2008, range of sampling years) and 497 bigeye (1971-2007) in the central north (Hawaii), and 103 skipjack in the northwest (along the Asian coasts, 1997-2011). The Pacific dataset also includes 627 Hg data results for tropical tunas (336 yellowfin, 127 bigeye and 164 skipjack) from the southwest from 2001 to 2021. In the Atlantic Ocean, the dataset includes 76 yellowfin in the tropical northwest (1999-2012), and 533 Hg data (301 yellowfin and 232 bigeye) in the central east (1971-2022). In the western Indian Ocean, 562 Hg data in tunas (223 yellowfin, 186 bigeye, and 153 skipjack) were compiled from 2001 to 2022. Published data¹⁻⁶ were obtained directly from Drevnick and Brooks⁷ and Peterson et al.⁸, or from contributions by the original authors⁹⁻¹⁴.

All tuna samples were collected onboard commercial, recreational, and scientific fishing vessels by multiple research programs. For each fish, a white muscle sample was collected, and metadata (i.e., sampling year, average or precise catch location, total weight and/or fork length (FL)) were also

provided. When only fish weight was available^{1,2,4–6,8}, fish mass was converted into fish size (as fork length) to allow size-based comparison between samples, using species- and ocean-specific length-weight relationships^{15,16}.

Total mercury concentrations analysis: Total Hg concentrations were measured on homogenized tuna muscle samples in different study-specific laboratories, with laboratory-specific reference standards to ensure measurements accuracy and traceability. For half of the samples (~ 45%), total Hg concentrations were measured by hot-plate acid digestion followed by cold vapor atomic fluorescence spectroscopy or cold vapor atomic absorption^{1,2,4–6,9,12,14,17}. For the rest of the samples (~ 55%), total Hg concentrations were measured by thermal decomposition, gold amalgamation, and atomic absorption spectrometry (DMA-80, Milestone, Italy)^{10,11,14}. This includes 1,058 newly acquired Hg data in different laboratories: at GET (Toulouse, France; $n = 569$), SFA (Victoria, Seychelles; $n = 469$), and FWC-FWRI (Melbourne, Florida, USA; $n = 20$). Total Hg concentrations were obtained either on bulk powdered samples ($n = 2,800$) or on historic lipid-free samples in the eastern central Atlantic Ocean ($n = 110$, samples in 2003, 2013 and 2014). Lipid removal with neutral solvent has been shown to have no effect on total Hg concentrations in tropical tunas¹⁸, allowing us to compare bulk and lipid-free samples to explore the temporal variability of tuna Hg content in the eastern central Atlantic ocean. When total Hg concentrations were obtained on fresh samples, we converted Hg concentrations assuming an average moisture value of 70% in white muscle of tropical tunas¹⁹, so that all total Hg concentrations are expressed on a dry weight (dw) basis.

As Hg is known to naturally bioaccumulate with fish length, we fitted a power-law relationship ($\log(Hg) = a \times (FL - c)^b - d$) between log-transformed Hg concentrations and fish length (FL) to remove the length effect when exploring temporal variability. Power-law relationships were fitted for each species and ocean region, all years combined (SI Fig. S2). Residuals from the length-based Hg models (i.e., observed values minus predicted values) were extracted and used to calculate length-standardized Hg concentrations, thereafter defined as “standardized Hg concentrations”. Mercury standardization was performed at 100 cm FL for bigeye and yellowfin, and 70 cm FL for skipjack.

Nitrogen isotope analysis: Measured in the tissues of consumers, $\delta^{15}\text{N}$ values are used to estimate trophic position as they increase predictably between prey and consumer²⁰. We assembled 1,535 tuna muscle $\delta^{15}\text{N}$ values globally, corresponding to 599 samples in the southwestern Pacific (2001–2021), 501 samples in the western Indian (2001–2022), and 435 samples in the eastern central Atlantic (2002–2022). For each sample, $\delta^{15}\text{N}$ values were measured on homogenized freeze-dried samples packed in tin cups and analysed in different study-specific laboratories. Most of the isotope data ($n = 1,078$, 70%), including the 521 newly acquired ones, were obtained at the Union College Stable Isotope Laboratory (Schenectady, New York, USA) using a Costech elemental analyzer coupled to a Thermo Advantage isotope ratio mass spectrometer with a ConFlo 3. About 23% of the isotope data ($n = 355$) were measured at the LIENSs stable isotope facility (La Rochelle, France) using a Flash EA 1112 elemental analyzer coupled to a Delta V Advantage ratio mass spectrometer with a Conflo IV^{21,22}. The

rest of the $\delta^{15}\text{N}$ values ($n = 102$, ~7%) were obtained using a Europa Scientific ANCANT 20-20 stable isotope analyzer with ANCA-NT Solid/Liquid Preparation Module²³. All results were reported in the δ unit notation and expressed as parts per thousand (‰) relative to international standards (atmospheric N₂ for nitrogen). Depending on the laboratory, a combination of certified and/or in-house reference materials were used to determine that uncertainty was below 0.2‰. Carbon stable isotope values were corrected for lipids, either with chemical extraction ($n = 457$), or using a mass balance equation for samples with elevated lipid content (C:N > 3.5, $n = 22$), with parameters derived from Atlantic bluefin tuna muscle²⁴.

Future mercury emissions scenarios: We used a previously published global biogeochemical cycle model^{25,26} (available at <https://github.com/SunderlandLab/gbc-boxmodel>) to simulate the impacts of global anthropogenic emissions on environmental Hg. The seven-box model allows full coupling of the ocean, atmosphere, and terrestrial reservoirs and therefore takes into account Hg re-emissions from the land and the ocean, estimated to represent ~2/3 of the global Hg emissions. The seven reservoirs include the atmosphere, the surface ocean (extending to the base of the mixed layer, ~50 m), the subsurface ocean (extending to the depth of the permanent thermocline, ~1500 m), the deep ocean (extending to the sea floor), and terrestrial ecosystems (i.e., fast terrestrial, slow and armored soils). Mercury cycles between reservoirs and is ultimately removed by burial in marine sediments. The model was driven by 2000 BCE (Before Common Era) to 2015 CE (Common Era) primary anthropogenic emissions from Streets et al.^{27–30}. We considered three contrasted emission scenarios, as defined in Angot et al.³¹, when simulating future emissions for the 2016–2100 period in order to investigate the time lag responses of each reservoir to changing emissions scenarios. Briefly, the Current Policy scenario projects that annual Hg emissions will slightly increase in 2035 (+3.02 Mg.y⁻¹). The more stringent New Policy scenario indicates that annual emissions will significantly decrease by 2035 (-32.7 Mg.y⁻¹), as developed in Pacyna et al.³². Finally, the Maximum Feasible Scenario assumes that all countries reach the highest feasible reduction efficiency in each emission sector, leading to a dramatic decrease of annual anthropogenic Hg emissions (-59.9 Mg.y⁻¹).

Statistical analyses: As required by the Hg research community when investigating Hg temporal trends in biota, we examined the adequacy of each time series, i.e., we compared the time series ability to detect trends and at the same time indicate whether trend detection is justified for the time series^{33,34}. Adequacy is defined as the number of actual monitoring years in a time series divided by the number of sampling years required to detect a 5% annual change in tuna Hg concentrations with a significance level of $p < 0.05$ and 80% statistical power³⁵. A ratio ≥ 1 implies that a time series is adequate to investigate temporal trends over the entire time period. Among the 12 time series in our global dataset, five had an adequacy ≥ 1 . These were yellowfin and skipjack in the southwestern Pacific, yellowfin and bigeye in the western Indian, and bigeye in the eastern central Atlantic (SI Appendix Fig. S3).

To allow comparison among all the time series while accounting for their distinct adequacy values, we investigated inter-annual differences of standardized Hg concentrations in tunas per species and ocean region, using Kruskal-Wallis tests, followed by a post-hoc Dunn test with a Bonferroni correction of p -values. This approach avoids finding significant temporal trends between samples that

are sometimes more than 20 years apart, but highlights patterns of Hg concentrations between old and recent periods (defined arbitrarily by a minimum of three consecutive years).

The adequacy calculation was assessed with the PIA software³⁶, and the Hg box model was run on MATLAB R2023a³⁷. All other statistical analyses were performed with the statistical open source R software 3.6.1³⁸.

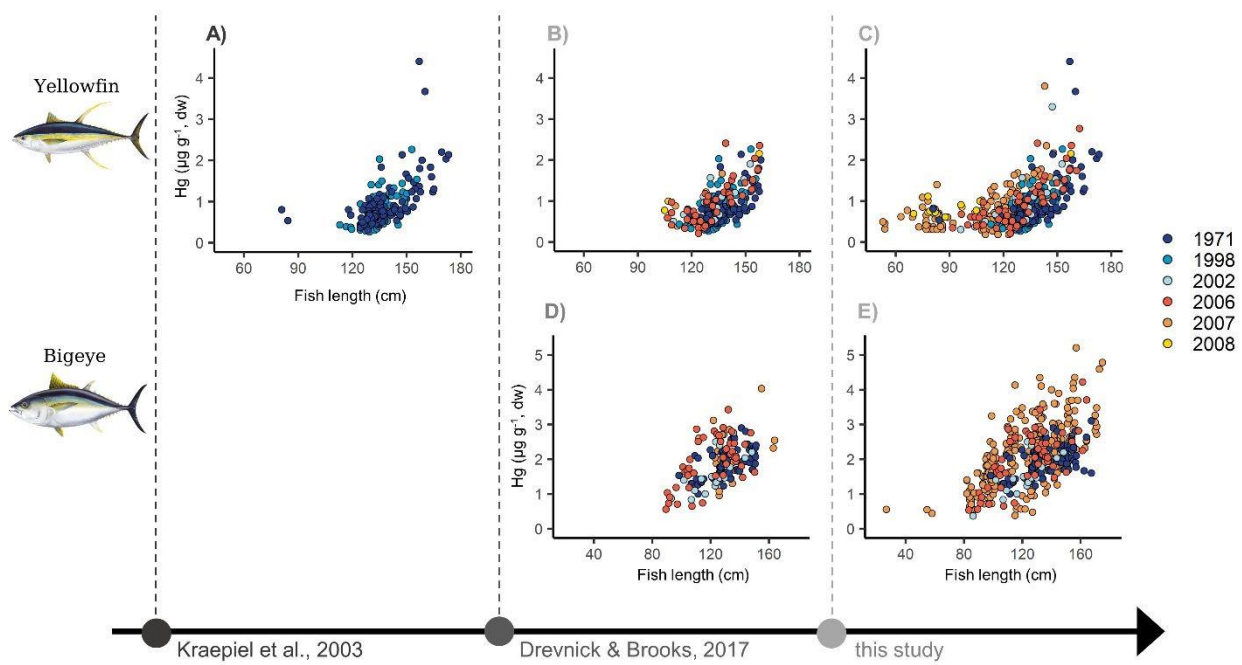


Figure S1. Chronological development of research effort aimed at investigating temporal trends in mercury concentrations in yellowfin and bigeye tunas in the central north Pacific Ocean. Tunas illustrations were created by Les Hata, @SPC.

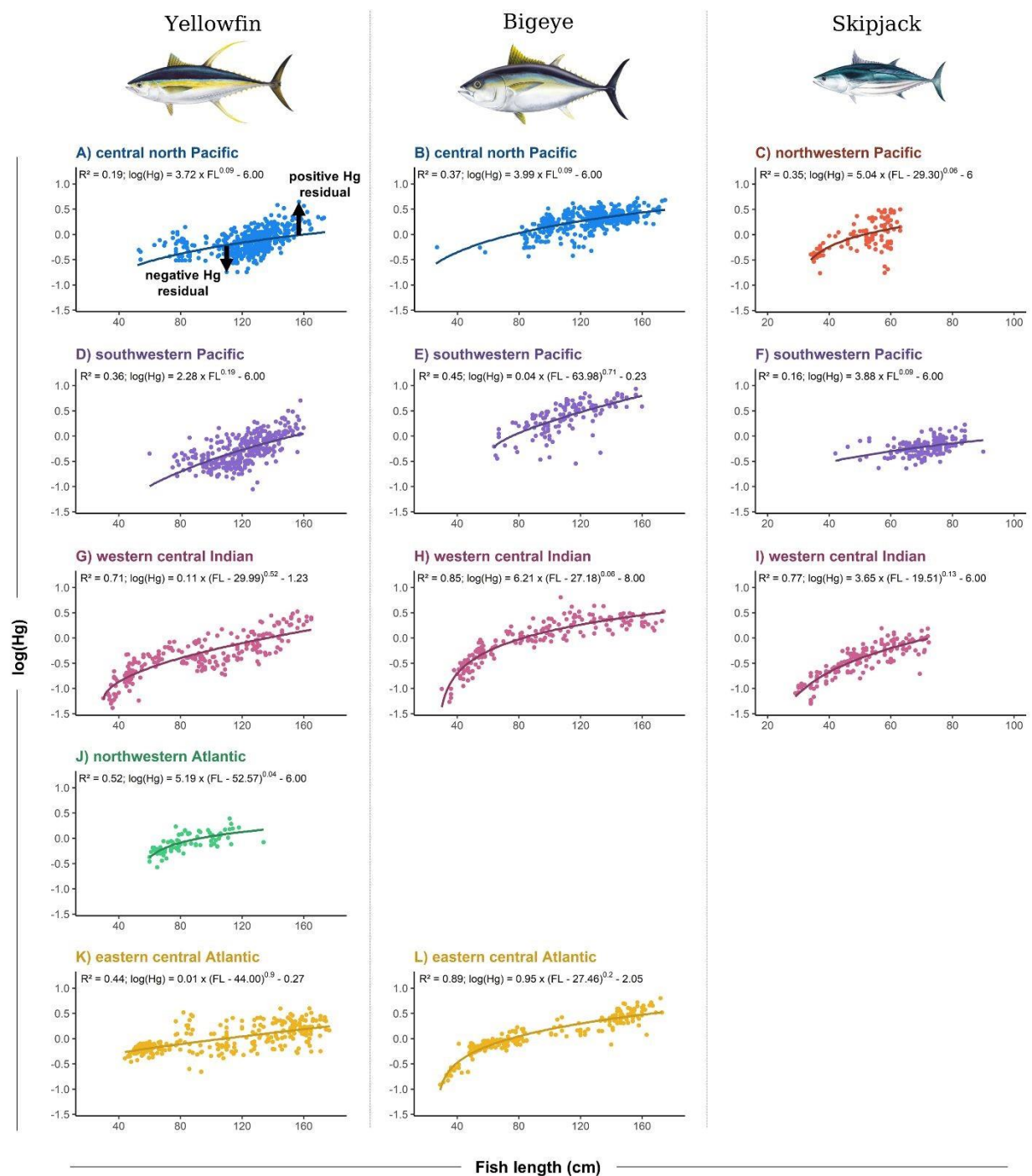


Figure S2. Length-standardization of tuna mercury concentrations. Power-law relationships between log-transformed observed mercury concentrations ($\log(\text{Hg})$) and fork length (FL), all years combined, for **A)** yellowfin, and **B)** bigeye from the central north Pacific, **C)** skipjack from the northwestern Pacific, **D)** yellowfin, **E)** bigeye, and **F)** skipjack from the southwestern Pacific, **G)**, yellowfin, **H)** bigeye, and **I)** skipjack from the western Indian, **J)** yellowfin from the northwestern Atlantic, and **K)** yellowfin, and **L)** bigeye from the eastern central Atlantic. The black arrows in A) symbolize the calculation of positive and negative Hg residuals. Tunas illustrations were created by Les Hata, @SPC.

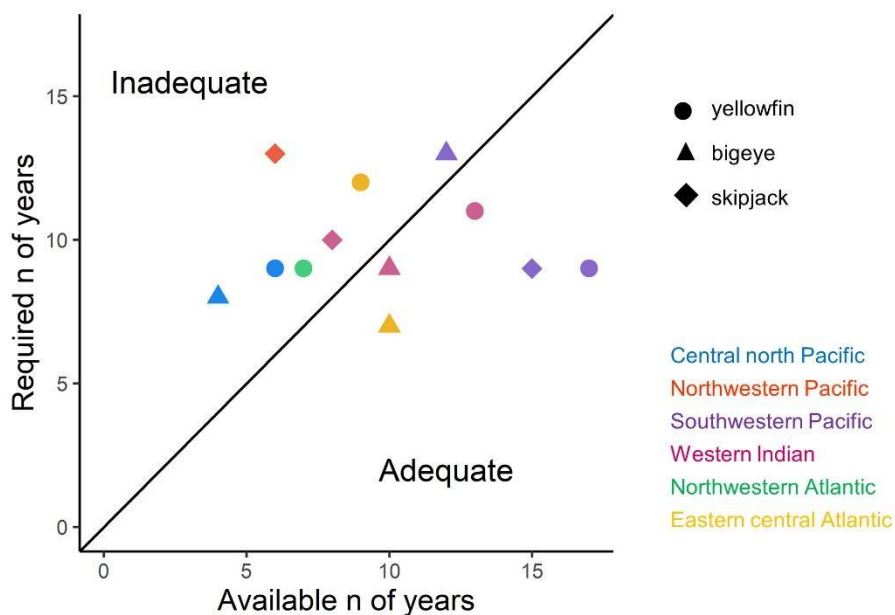


Figure S3. Statistical power of global time series of mercury concentrations in tunas. Adequacy values of mercury (Hg) time series data in skipjack (diamonds), yellowfin (dots), and bigeye (triangles) in the central north Pacific (blue), northwestern Pacific (red), southwestern Pacific (purple), western Indian (pink), northwestern Atlantic (green) and eastern central Atlantic (yellow). Adequacy to detect an annual change of 5% was calculated following the methods of Bignert et al.³⁵, considering a significance level of $p < 0.05$ and 80% statistical power. Datasets falling within the lower right portion of the graph are more than adequate in terms of statistical power, while those in the upper left portion are inadequate.

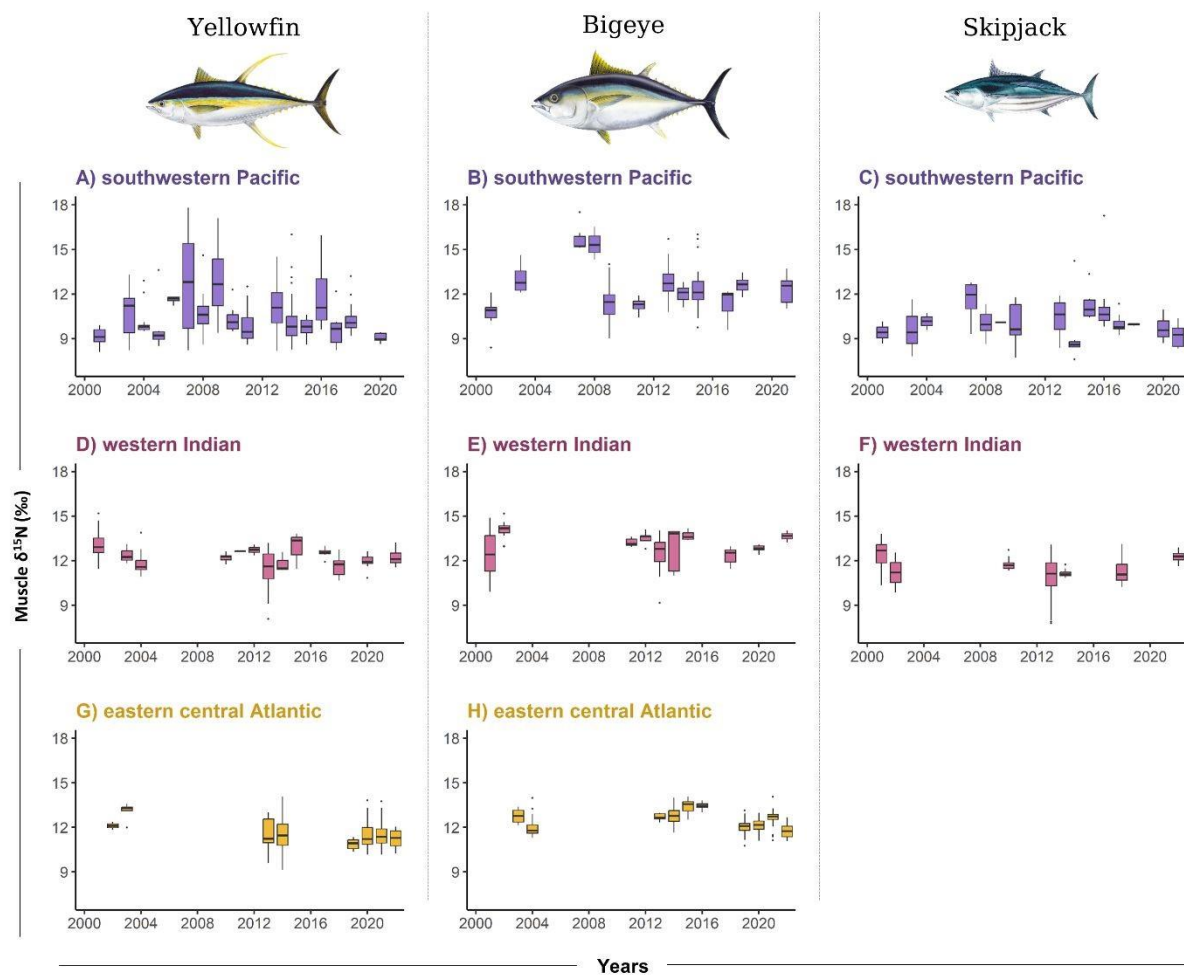


Figure S4. Temporal variability of nitrogen isotope values in tunas. Boxplots of nitrogen isotope values ($\delta^{15}\text{N}$, ‰) measured in muscle samples of **A)** yellowfin, **B)** bigeye, and **C)** skipjack in the southwestern Pacific (2001-2021), **D)** yellowfin, **E)** bigeye, and **F)** skipjack in the western Indian (2001-2022), and **G)** yellowfin and **H)** bigeye in the eastern central Atlantic (2003-2022). For all tuna species and ocean regions, the year-to-year comparison indicates no significant difference between old and recent $\delta^{15}\text{N}$ values, suggesting stable tuna trophic position over the study period. Tunas illustrations were created by Les Hata, @SPC.

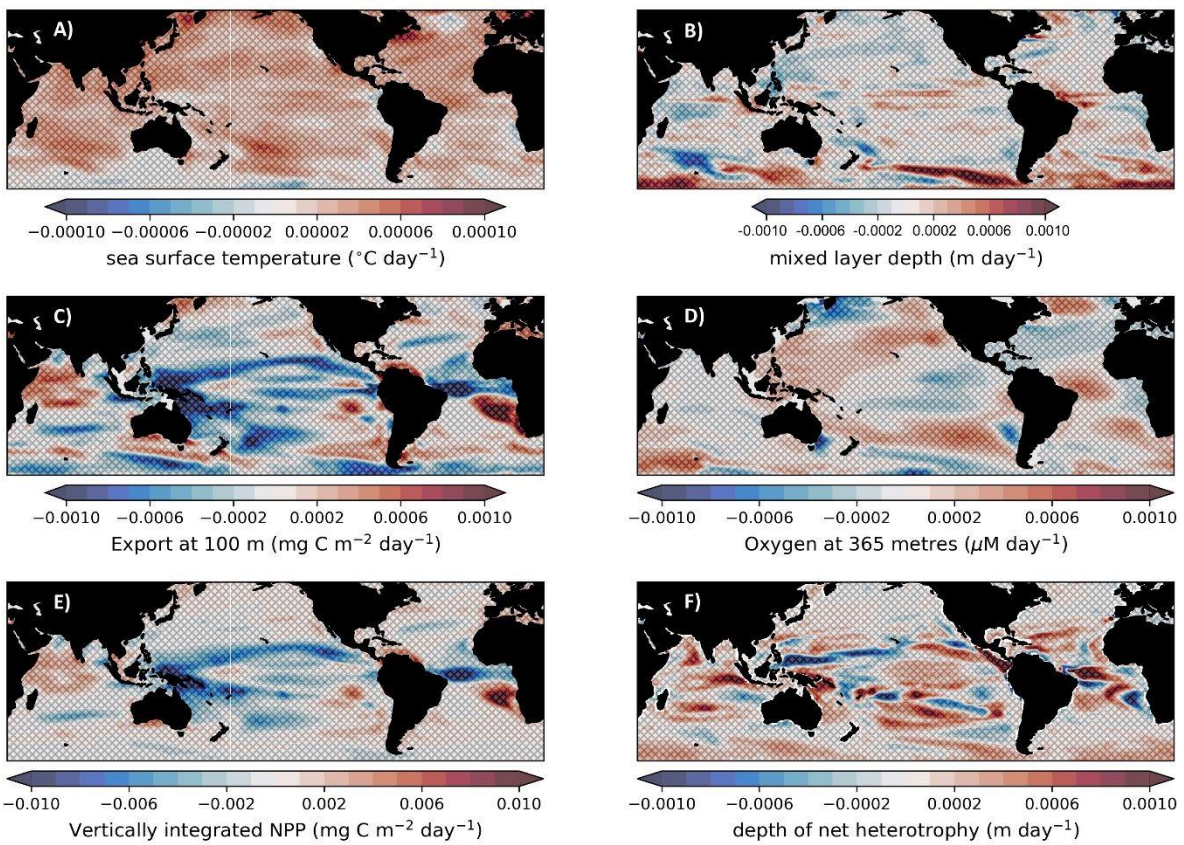


Figure S5. Temporal variability of oceanic variables suspected to drive *in situ* methylmercury production. The colour shading represents the linear trends from 1971 to 2022 of **A**) sea surface temperature ($^{\circ}\text{C day}^{-1}$), **B**) mixed layer depth (m day^{-1}), **C**) carbon export at 100m ($\text{mg C m}^{-2} \text{ day}^{-1}$), **D**) oxygen concentrations in subsurface waters ($\mu\text{M day}^{-1}$), **E**) vertically integrated net primary production (NPP) ($\text{mg C m}^{-2} \text{ day}^{-1}$), and **F**) depth of net heterotrophy (m day^{-1}), estimated by the biogeochemical model NEMO-PISCES³⁹. Linear trends were calculated on monthly anomalies, i.e., from monthly mean outputs with average monthly values subtracted. Crossed stippling shows where the standard deviation is greater than the linear trend from 1971 to 2022. None of the six variable shows any long-term trend that exceed one standard deviation, suggesting that for all variables, inter-annual variability is more important than the long-term trend.

Table S1. Summary of tuna samples collected in the global ocean and analysed for total mercury concentrations and stable isotope values. n_{THg} and $n_{\delta^{15}N}$ give the number of samples analysed in total mercury (THg) concentrations, and nitrogen isotope values ($\delta^{15}N$), respectively. Fish length correspond to fork length (cm) measured during tuna sampling, or calculated from whole fish weight (symbolised by *) using species- and ocean- specific length-weight relationships ^{15,16}.

Ocean area	Species	Sampling year	n_{THg}	Fish length (cm) mean ± sd	THg ($\mu\text{g.g}^{-1}$, dw) mean ± sd	References for THg	$n_{\delta^{15}N}$	$\delta^{15}N$ (%) mean ± sd	References for $\delta^{15}N$ values
Central north Pacific (Hawaii)	yellowfin	1971	122	137 ± 13 *	0.918 ± 0.573	1,6	-	-	-
		1998	104	133 ± 8 *	0.707 ± 0.369	5	-	-	-
		2002	20	129 ± 15 *	1.023 ± 0.686	2	-	-	-
		2006	50	130 ± 18 *	1.012 ± 0.588	4	-	-	-
		2007	200	113 ± 19	0.733 ± 0.444	^{10, 11, 12, this study}	-	-	-
		2008	16	95 ± 22	0.891 ± 0.380	10, 11	-	-	-
	bigeye	1971	104	136 ± 15 *	1.942 ± 0.425	1	-	-	-
		2002	20	120 ± 16 *	1.572 ± 0.618	2	-	-	-
		2006	50	124 ± 21 *	2.005 ± 0.820	4	-	-	-
		2007	323	123 ± 24	2.140 ± 0.851	^{10, 11, 12, this study}	-	-	-
North western Pacific (Asian coasts)	skipjack	1997	8	59 ± 1	0.507 ± 0.256	17	-	-	-
		1998	25	54 ± 5	0.809 ± 0.324	17	-	-	-
		1999	46	49 ± 11	1.328 ± 0.917	17	-	-	-
		2000	7	48 ± 1	1.309 ± 0.504	17	-	-	-
		2007	10	58 ± 2	2.138 ± 0.702	17	-	-	-
		2011	7	46 ± 1	0.656 ± 0.130	this study	-	-	-
South western Pacific (New Caledonia and Fiji)	yellowfin	2001	25	131 ± 5	0.631 ± 0.201	14	25	9.12 ± 0.57	14,40
		2003	13	115 ± 20	0.504 ± 0.812	14	13	10.84 ± 1.63	14,40
		2004	17	101 ± 15	0.508 ± 0.295	14	17	10.08 ± 0.94	14,40

	2005	11	108 ± 7	0.323 ± 0.095	14	11	9.52 ± 1.39	14,40
	2006	7	117 ± 13	0.729 ± 0.252	14	7	11.63 ± 0.22	14,40
	2007	29	108 ± 14	0.304 ± 0.141	14	29	12.54 ± 2.99	14,40
	2008	30	124 ± 13	0.849 ± 0.427	14	30	10.65 ± 1.15	14,40

Ocean area	Species	Sampling year	n _{THg}	Fish length (cm) mean ± sd	THg ($\mu\text{g.g}^{-1}$, dw) mean ± sd	References for THg	n _{δ15N}	δ ¹⁵ N (‰) mean ± sd	References for δ ¹⁵ N values
South western Pacific (New Caledonia and Fiji)	yellowfin	2009	16	128 ± 23	1.075 ± 0.764	14	16	12.81 ± 2.22	14,40
		2010	8	108 ± 18	0.411 ± 0.286	14	8	10.33 ± 0.94	14,40
		2011	14	126 ± 19	0.974 ± 1.260	14	14	9.87 ± 1.20	14,40
		2013	52	129 ± 15	0.752 ± 0.565	14	52	11.04 ± 1.36	14,40
		2014	40	118 ± 21	0.619 ± 0.450	14	40	10.16 ± 1.59	14,40
		2015	11	137 ± 9	0.727 ± 0.246	14	11	9.78 ± 0.61	14,40
		2016	10	124 ± 10	0.830 ± 0.356	14	10	11.73 ± 1.99	14
		2017	14	119 ± 21	0.513 ± 0.385	14	14	9.56 ± 1.30	14
		2018	30	129 ± 15	0.779 ± 0.448	14	30	10.25 ± 0.86	14
		2020	9	103 ± 18	0.574 ± 0.339	this study	9	9.10 ± 0.30	this study
	bigeye	2001	13	103 ± 12	2.989 ± 1.409	14	13	10.70 ± 0.84	14,40
		2003	4	126 ± 20	3.758 ± 2.293	14	4	13.05 ± 1.14	14,40
		2007	6	81 ± 15	0.644 ± 0.226	14	6	15.72 ± 0.95	14,40
		2008	3	99 ± 9	1.377 ± 0.660	this study	3	15.37 ± 1.10	this study
		2009	14	111 ± 25	3.069 ± 2.412	14	14	11.50 ± 1.55	14,40
		2011	4	125 ± 12	2.947 ± 0.895	14	4	11.23 ± 0.62	14,40
		2013	27	101 ± 24	2.201 ± 1.431	¹⁴ , this study	24	12.84 ± 1.06	14,40
		2014	14	106 ± 25	2.384 ± 1.176	14	14	12.04 ± 0.54	14,40

	2015	23	111 ± 15	2.658 ± 1.139	¹⁴	23	12.39 ± 1.56	^{14,40}
	2017	5	110 ± 17	3.342 ± 2.440	¹⁴	5	11.32 ± 1.10	¹⁴
	2018	9	131 ± 15	4.558 ± 1.935	¹⁴	9	12.67 ± 0.55	¹⁴
	2021	8	121 ± 6	4.682 ± 1.038	this study	8	12.29 ± 0.96	this study
skipjack	2001	2	78 ± 1	0.669 ± 0.069	this study	2	9.42 ± 1.04	this study
	2003	19	68 ± 7	0.544 ± 0.131	¹⁴	19	9.64 ± 1.15	¹⁴
	2004	2	56 ± 8	0.409 ± 0.102	this study	2	10.16 ± 0.81	this study
	2007	6	71 ± 3	0.641 ± 0.316	¹⁴	6	11.58 ± 1.35	¹⁴
	2008	11	71 ± 3	0.652 ± 0.124	¹⁴	10	10.05 ± 0.82	¹⁴

Ocean area	Species	Sampling year	n _{THg}	Fish length (cm) mean ± sd	THg (µg.g ⁻¹ , dw) mean ± sd	References for THg	n _{δ15N}	δ ¹⁵ N (‰) mean ± sd	References for δ ¹⁵ N values
South western Pacific (New Caledonia and Fiji)	skipjack	2009	8	68 ± 8	0.645 ± 0.351	¹⁴	1	10.08	¹⁴
		2010	13	71 ± 8	0.621 ± 0.225	¹⁴	13	9.90 ± 1.24	¹⁴
		2013	25	73 ± 10	0.644 ± 0.213	¹⁴	16	10.51 ± 1.06	¹⁴
		2014	13	74 ± 6	0.692 ± 0.311	¹⁴	7	9.26 ± 2.22	¹⁴
		2015	14	73 ± 4	0.601 ± 0.283	¹⁴	10	11.19 ± 0.90	¹⁴
		2016	22	71 ± 9	0.682 ± 0.223	¹⁴	22	10.91 ± 1.51	¹⁴
		2017	11	73 ± 7	0.746 ± 0.348	¹⁴	10	9.97 ± 0.62	¹⁴
		2018	2	75 ± 8	1.150 ± 0.433	this study	2	9.95 ± 0.13	this study
		2020	11	73 ± 7	0.746 ± 0.348	this study	10	9.71 ± 0.77	this study
		2021	6	71 ± 5	0.647 ± 0.222	this study	6	9.21 ± 0.84	this study
Western Indian (Seychelles and Mozambique Channel)	yellowfin	2001	15	96 ± 38	0.615 ± 0.445	¹³	15	13.15 ± 1.04	²³
		2003	3	112 ± 33	0.601 ± 0.230	¹³	3	12.39 ± 0.65	²³
		2004	23	108 ± 17	0.543 ± 0.367	¹³ , this study	22	11.76 ± 0.66	²³

	2010	9	92 ± 52	0.954 ± 0.819	this study	9	12.22 ± 0.28	this study
	2011	2	140 ± 1	2.268 ± 0.730	this study	2	12.65 ± 0.08	this study
	2012	5	153 ± 4	2.493 ± 0.340	this study	4	12.73 ± 0.31	this study
	2013	67	92 ± 33	0.731 ± 0.638	this study	67	11.55 ± 1.12	²¹
	2014	3	76 ± 75	0.934 ± 1.481	this study	3	11.81 ± 0.67	this study
	2015	3	164 ± 2	2.340 ± 0.200	this study	3	12.86 ± 1.26	this study
	2017	13	112 ± 29	0.760 ± 0.428	this study	10	12.57 ± 0.29	this study
	2018	50	52 ± 24	0.229 ± 0.196	this study	18	11.62 ± 0.58	this study
	2020	10	131 ± 17	0.708 ± 0.249	this study	10	11.93 ± 0.49	this study
	2022	20	110 ± 22	0.526 ± 0.261	this study	19	12.21 ± 0.49	this study
bigeye	2001	19	67 ± 31	0.552 ± 0.476	this study	19	12.53 ± 1.42	²³
	2002	11	131 ± 26	1.650 ± 0.515	this study	11	14.06 ± 0.65	²³
	2011	10	105 ± 26	1.851 ± 0.611	this study	10	13.23 ± 0.25	this study
	2012	6	142 ± 10	1.780 ± 0.266	this study	5	13.51 ± 0.49	this study

Ocean area	Species	Sampling year	n_{THg}	Fish length (cm) mean \pm sd	THg ($\mu\text{g.g}^{-1}$, dw) mean \pm sd	References for THg	$n_{\delta^{15}\text{N}}$	$\delta^{15}\text{N} (\text{\textperthousand})$ mean \pm sd	References for $\delta^{15}\text{N}$ values
Western Indian (Seychelles and Mozambique Channel)	bigeye	2013	64	84 ± 38	1.022 ± 0.863	this study	64	12.60 ± 0.89	²¹
		2014	8	109 ± 63	1.876 ± 1.496	this study	7	12.77 ± 1.48	this study
		2015	8	162 ± 8	2.238 ± 0.367	this study	8	13.69 ± 0.31	this study
		2018	33	59 ± 14	0.685 ± 0.412	this study	16	12.29 ± 0.53	this study
		2020	10	99 ± 4	1.278 ± 0.349	this study	8	12.83 ± 0.22	this study
		2022	17	115 ± 14	3.101 ± 1.040	this study	17	13.67 ± 0.24	this study
	skipjack	2001	30	54 ± 11	0.489 ± 0.263	this study	30	12.41 ± 0.94	²³
		2002	2	47 ± 1	0.403 ± 0.276	this study	2	11.21 ± 1.90	²³

		2010	8	46 ± 9	0.563 ± 0.555	this study	8	11.79 ± 0.48	this study
		2013	67	53 ± 11	0.553 ± 0.331	this study	66	10.97 ± 1.18	²¹
		2014	8	34 ± 4	0.135 ± 0.070	this study	8	11.18 ± 0.30	this study
		2015	2	46 ± 16	0.482 ± 0.398	this study	2	12.01 ± 0.19	this study
		2018	20	46 ± 11	0.312 ± 0.236	this study	19	11.33 ± 0.86	this study
		2022	16	61 ± 10	0.589 ± 0.287	this study	16	12.26 ± 0.35	this study
North western Atlantic (tropical US coasts)	yellowfin	1999	33	88 ± 15	1.149 ± 0.417	⁹	-	-	-
		2000	3	105 ± 34	0.654 ± 0.257	⁹	-	-	-
		2001	14	76 ± 19	0.633 ± 0.337	⁹	-	-	-
		2002	6	80 ± 14	0.663 ± 0.125	⁹	-	-	-
		2005	5	67 ± 2	0.581 ± 0.059	this study	-	-	-
		2006	8	100 ± 5	1.033 ± 0.232	this study	-	-	-
		2011	7	86 ± 13	0.733 ± 0.269	this study	-	-	-
Eastern central Atlantic (Gulf of Guinea)	yellowfin	1971	77	$142 \pm 31 *$	1.431 ± 0.761	³	-	-	-
		2002	2	128 ± 25	2.273 ± 2.338	this study	2	12.11 ± 0.38	this study
		2003	6	68 ± 13	0.648 ± 0.132	this study	6	13.10 ± 0.57	this study
		2013	46	122 ± 21	1.225 ± 0.663	this study	45	11.52 ± 0.99	²²
		2014	58	130 ± 31	1.545 ± 0.787	this study	57	11.51 ± 1.01	²²
		2019	6	56 ± 4	0.659 ± 0.079	this study	6	10.87 ± 0.40	this study

Ocean area	Species	Sampling year	n_{THg}	Fish length (cm) mean \pm sd	THg ($\mu\text{g.g}^{-1}$, dw) mean \pm sd	References for THg	$n_{\delta^{15}\text{N}}$	$\delta^{15}\text{N} (\text{‰})$ mean \pm sd	References for $\delta^{15}\text{N}$ values
Eastern central Atlantic (Gulf of Guinea)	yellowfin	2020	52	59 ± 10	0.670 ± 0.116	this study	52	11.47 ± 0.87	this study
		2021	39	60 ± 10	0.657 ± 0.116	this study	39	11.52 ± 0.83	this study
		2022	15	59 ± 5	0.626 ± 0.085	this study	15	11.23 ± 0.59	this study

bigeye	2003	6	42 ± 3	0.342 ± 0.222	this study	3	12.76 ± 0.51	this study
	2004	20	39 ± 12	0.300 ± 0.263	this study	20	12.03 ± 0.67	this study
	2013	9	149 ± 9	2.754 ± 1.039	this study	9	12.70 ± 0.22	²²
	2014	48	124 ± 29	2.123 ± 1.204	this study	47	12.73 ± 0.59	²²
	2015	19	150 ± 11	2.717 ± 0.950	this study	19	13.45 ± 0.41	this study
	2016	15	153 ± 10	3.393 ± 1.252	this study	15	13.44 ± 0.26	this study
	2019	36	60 ± 11	0.843 ± 0.317	this study	36	12.06 ± 0.45	this study
	2020	32	70 ± 9	0.848 ± 0.104	this study	32	12.13 ± 0.45	this study
	2021	28	61 ± 10	0.819 ± 0.273	this study	13	10.69 ± 0.84	this study
	2022	19	62 ± 5	0.761 ± 0.092	this study	19	11.79 ± 0.48	this study

Table S2. Global review of atmospheric mercury monitoring sites. List of long-term monitoring sites measuring atmospheric mercury (Hg) concentrations, updated from the latest technical report of the Global Mercury Assessment⁴¹. This list may not be exhaustive and does not provide information about whether the stations are currently operational.

Monitoring site	Country	Elevation (m)	Longitude (°)	Latitude (°)	Starting year	References
Villum Research Station	Greenland	30	-16.61	81.58	1999	42,43
Pallas	Finland	340	24.24	68.00	1996	43,44
Råö	Sweden	5	11.91	57.39	2012	45
Mace Head	Ireland	5	-9.91	53.33	1995	46
Listvyanka	Russia	670	104.89	51.85	2012	45
Col Margherita	Italy	2545	11.79	46.37	2012	45
Longobucco	Italy	1379	16.61	39.39	2012	45
Minamata	Japan	20	130.40	32.23	2011	45
Ev-K2	Nepal	5050	86.81	27.96	2012	45
Sisal	Mexico	7	-90.05	21.16	2013	45
Calhau	Cape Verde	10	-24.87	16.86	2011	45
Kodaicanal	India	2333	77.47	10.23	2012	45
Nieuw Nickerie	Suriname	1	-57.04	5.96	2012	45
Manaus	Brazil	110	-59.97	-2.89	2012	45
Amsterdam Island	French Southern and Antarctic Lands	70	77.55	-37.80	2012	47-50
Cape Point	South Africa	230	18.49	-34.35	1995	49-51
Bariloche	Argentina	801	-71.42	-41.13	2012	52
Dumont d'Urville	Antarctica	40	140.00	-66.66	2012	53,54
Concordia Station	Antarctica	3220	123.35	-75.10	2012	53,55
Denali National Park	United States, AK	661	-148.97	63.72	2014	43
Birmingham	United States, AL	200	-86.81	33.55	2009	56
Elkhorn Slough	United States, CA	15	-121.78	36.81	2010	56
Pensacola	United States, FL	45	-87.38	30.55	2009	56,57
Yorkville	United States, GA	395	-85.05	33.93	2009	56
Mauna Loa	United States, HI	3399	-155.58	19.54	2010	56
Piney Reservoir	United States, MD	769	-79.01	39.71	2008	56
Beltsville	United States, MD	46	-76.82	39.03	2006	56

Presque Isle	United States, ME	165	-68.03	46.70	2014	58
Grand Bay NERR	United States, MS	2	-88.43	30.43	2006	56
Thompson Farm	United States, NH		-70.95	43.11	2009	56
Brigantine	United States, NJ	1	-74.45	39.46	2009	56
New Brunswick	United States, NJ	21	-74.42	40.47	2009	56
Elizabeth Lab	United States, NJ	11	-74.21	40.64	2009	56
Bronx	United States, NY	68	-73.88	40.87	2008	59
Huntington Wildlife	United States, NY	500	-74.22	43.97	2006	60
Rochester	United States, NY	136	-77.55	43.15	2007	61
Athens Super Site	United States, OH	275	-82.12	39.31	2004	62
South Bass Island	United States, OH	177	-82.83	41.66	2011	58
Stilwell	United States, OK	299	-94.67	35.75	2009	56
Antelope Island	United States, UT	1287	-112.02	41.05	2009	56
Salt Lake City	United States, UT	1297	-111.96	40.71	2008	56
Underhill	United States, VT	399	-72.87	44.53	2008	56,57
Horicon Marsh	United States, WI	287	-88.62	43.47	2011	56
Little Fox Lake	Canada, YK	-	-135.63	61.35	2007	43,63
Ucluelet	Canada, BC	-	-125.54	48.92	2010	57
Reifel Island	Canada, BC	-	-123.17	49.10	1999	63
Saturna	Canada, BC	-	-123.13	48.78	2009	57,63
Whistler	Canada, BC	-	-122.93	50.07	2008	57,63
Meadows	Canada, AB	-	-114.64	53.53	2005	63
Genesee	Canada, AB	-	-114.20	53.30	2004	63
Fort Chipewyan	Canada, AB	-	-111.12	58.78	2000	63
Esther	Canada, AB	-	-110.20	51.67	1998	63
Fort McKay South	Canada, AB	-	-111.64	57.15	2014	57
Patricia McInnis	Canada, AB	-	-111.48	56.75	2010	64
Bratt's Lake	Canada, SK	-	-104.71	50.20	2001	57,63
Flin Flon	Canada, MB	-	-101.88	54.77	2008	57,63
Burnt Island	Canada, ON	-	-82.95	45.81	1998	63
Egbert	Canada, ON	-	-79.78	44.23	1996	57,63
Kuujjuarapik	Canada, QC	-	-77.73	55.30	1999	63
Point Petre	Canada, ON	-	-77.15	43.84	1996	63

Saint Anicet	Canada, QC	-	-74.03	45.20	1994	57,63
Saint Andrews	Canada, NB	-	-67.08	45.08	1996	63
Kejimkujik	Canada, NS	-	-65.21	44.43	1996	63
Mingan	Canada, QC	-	-64.17	50.27	1997	57,63
Southampton	Canada, PE	-	-62.58	46.39	2005	63
Alert	Canada, NU	-	-62.33	82.50	1995	43
An-myun	South Korea	46	126.32	36.53	2004	65
Cape Hedo	Japan	60	128.25	26.86	2007	66
Chongqing	China	350	106.50	29.60	2006	67,68
Guangzhou	China	60	113.36	23.12	2010	68
Jeju Island	South Korea	67	126.16	33.29	2006	69
Lulin	Chinese Taipei	2862	120.92	23.51	2006	70
Miyun	China	220	116.78	40.48	2008	68
Mount Ailao	China	2450	101.02	24.53	2011	68
Mount Changbai	China	740	128.11	42.40	2008	68
Mount Damei	China	550	121.57	29.63	2011	68
Mount Dinghu	China	700	112.55	23.16	2009	68
Mount Gongga	China	1640	102.12	29.65	2005	68
Mount Leigong	China	2178	108.20	26.39	2008	68
Mount Walinguan	China	3816	100.90	36.29	2007	68,71
Seoul	South Korea	77	126.93	37.61	1987	72
Shanghai	China	19	121.54	31.23	2004	68
Shangri-La	China	3580	99.73	28.02	2009	68
Tae-An	South Korea	23	126.13	36.74	2014	-
Tokai-mura	Japan	15	140.36	36.27	2005	73
Xiamen	China	7	118.05	24.60	2012	68,74
Yongheung Island	South Korea	32	126.46	37.28	2013	75
Waldhof	Germany	74	10.76	52.80	2006	46
Harwell	United Kingdom	137	-1.33	51.57	2012	76
Auchencorth Moss	United Kingdom	260	-3.24	55.79	2009	77

Zeppelin	Norway/Svalbard	474	11.88	78.91	2000	43,46
Amderma	Russia	49	61.62	69.72	2001	43,46
Andoya	Norway	380	16.01	69.28	2010	43,46
Iskrba	Italy	520	14.86	45.56	2012	45
Troll	Antarctica	1275	2.53	-72.01	2007	50
Cape Grim	Australia	-	144.68	-40.68	2011	50
Gunn Point	Australia	-	131.04	-12.25	2014	78
Maïdo mountain observatory	Reunion Island, France	2160	55.83	-21.17	2017	79
LAMTO	Ivory Coast	-	-5.03	6.5	2023	A. Dommergue, personal communication

The comparison of Hg time series in tunas with existing atmospheric observation data shows that Hg data poorly match in space and/or time. In the northern hemisphere, where the existing atmospheric monitoring network is the most developed ($n = 99$, 90% of the total number of monitoring stations), the earliest stations in the geographic vicinity of our tuna samples started in the second half of the 2000s (i.e., Mauna Loa (Hawaii) in 2010 for the central north Pacific; Chinese stations from 2004 for the northwestern Pacific; and Pensacola (Florida) in 2009 for the northwestern Atlantic) while most of our tuna Hg data end at the beginning of the 2000s. In the southern hemisphere, where we have tuna Hg data over the last two decades, air monitoring stations of interest started too recently to evaluate how tuna Hg trends might relate to changes in atmospheric Hg concentrations (i.e., Maïdo mountain (Reunion Island) started in 2017 for the western Indian ⁷⁹; and LAMTO station (Ivory Coast) in 2023 for the eastern central Atlantic).

Table S3. Year-to-year comparisons of tuna mercury concentrations. Results of the post-hoc Dunn's tests on standardized mercury (Hg) concentrations for **A)** yellowfin and **B)** bigeye in the central north Pacific, **C)** skipjack in the northwestern Pacific, **D)** yellowfin, and **E)** bigeye in the southwestern Pacific, **F)** yellowfin, and **G)** bigeye in the western Indian, **H)** yellowfin in the tropical northwestern Atlantic, and **I)** bigeye in the eastern central Pacific. No Dunn tests were performed for standardized Hg concentrations in yellowfin in the eastern central Atlantic, and skipjack in the southwestern Pacific and the western Indian, as no significant differences were found among years in these three cases (Kruskal-Wallis test, $p > 0.05$).

A)Yellowfin in central north Pacific

	1998	2002	2006	2007	2008
1971	< 0.05	1.00	0.72	1.00	< 0.05
1998		< 0.05	< 0.05	< 0.05	< 0.05
2002					
2006			1.00	1.00	0.14
2007				1.00	< 0.05
B)					< 0.05

Bigeye in central north Pacific

	2002	2006	2007
1971	1.00	< 0.05	< 0.05
2002		0.09	< 0.05
2006			0.32

C)Skipjack in the northwestern Pacific

1998 1999 2000 2007 2011

D)

1997	1.00	< 0.05	< 0.05	< 0.05	1.00
1998		< 0.05	< 0.05	< 0.05	1.00
1999					
2000			1.00	1.00	0.10
2007				1.00	0.23
					< 0.05
2013	2014	2015	2016	2017	2020

Yellowfin in the southwestern Pacific

2003 2004 2005 2006 2007 2008 2009 2010 2011

2001	1.00	1.00	1.00	1.00	1.00	1.00	1.00	1.00	1.00	1.00	1.00	1.00	1.00	1.00	1.00	0.18
2003		0.08	1.00	0.63	1.00	0.06	< 0.05	1.00	1.00	1.00	1.00	1.00	0.22	1.00	1.00	0.25
2004			0.35	1.00	< 0.05	1.00	1.00	1.00	1.00	1.00	1.00	1.00	0.90	1.00	1.00	1.00
2005				1.00	1.00	0.32	0.22	1.00	1.00	1.00	1.00	1.00	0.70	1.00	1.00	0.74
2006					0.22	1.00	1.00	1.00	1.00	1.00	1.00	1.00	1.00	1.00	1.00	1.00
2007						< 0.05	< 0.05	1.00	1.00	1.00	0.92	1.00	< 0.05	1.00	0.09	0.05
2008							1.00	1.00	0.65	1.00	1.00	0.85	1.00	1.00	1.00	1.00
2009								1.00	1.00	0.63	1.00	1.00	0.56	1.00	1.00	1.00
2010									1.00	1.00	1.00	1.00	1.00	1.00	1.00	1.00
2011										1.00	1.00	1.00	1.00	1.00	1.00	1.00
2013											1.00	1.00	1.00	1.00	1.00	1.00
2014												1.00	1.00	1.00	1.00	1.00
2015													1.00	1.00	1.00	1.00
2016														1.00	1.00	1.00
2017															1.00	1.00
2018																1.00
E) Bigeye in the																

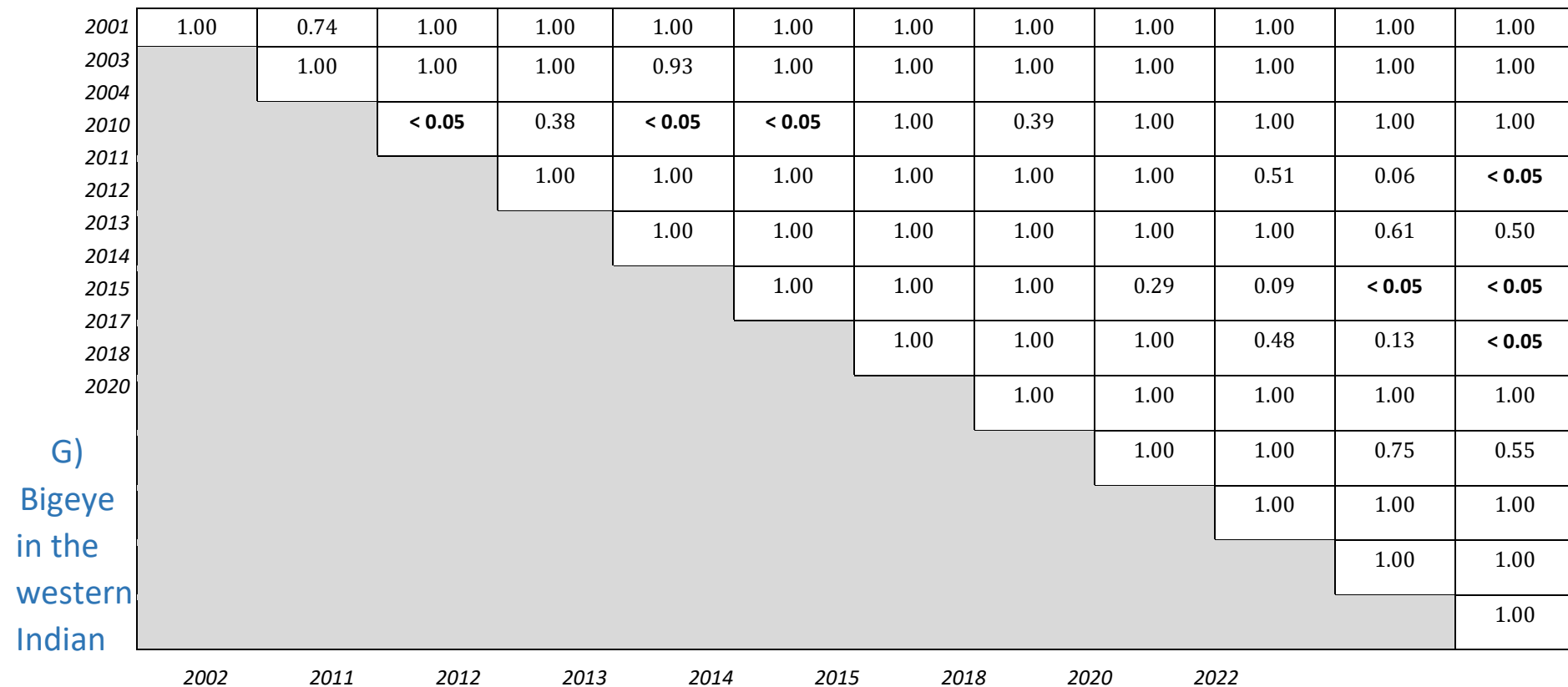
southwestern Pacific

2003 2007 2008 2009 2011 2013 2014 2015 2017 2018 2021

2001	1.00	< 0.05	0.63	1.00	1.00	1.00	1.00	1.00	1.00	1.00	1.00
2003		1.00	1.00	1.00	1.00	1.00	1.00	1.00	1.00	1.00	1.00
2007			1.00	0.88	1.00	0.72	1.00	0.85	0.84	0.22	< 0.05
2009				1.00	1.00	1.00	1.00	1.00	1.00	1.00	0.39
2011					1.00	1.00	1.00	1.00	1.00	1.00	1.00
2013						1.00	1.00	1.00	1.00	1.00	1.00
2014							1.00	1.00	1.00	1.00	0.86
2015								1.00	1.00	1.00	1.00
2017									1.00	1.00	1.00
2018										1.00	1.00
F)											1.00

Yellowfin in the western Indian

2003 2004 2010 2011 2012 2013 2014 2015 2017 2018 2020 2022



H)

2001	1.00	< 0.05	1.00	0.67	1.00	1.00	< 0.05	1.00	< 0.05
2002		0.16	1.00	1.00	1.00	1.00	0.07	1.00	< 0.05
2011			0.13	0.78	1.00	0.12	1.00	1.00	1.00
2012				1.00	1.00	1.00	0.09	1.00	< 0.05
2013					1.00	1.00	0.13	1.00	< 0.05
2014						1.00	1.00	1.00	
2015							0.07	1.00	< 0.05
2018								1.00	0.15
2020									< 0.05

Yellowfin in the
northwestern

Atlantic

	2000	2001	2002	2005	2006	2011
1999	< 0.05	< 0.05	0.17	1.00	0.26	< 0.05
2000		1.00	1.00	0.60	1.00	1.00
2001			1.00	1.00	1.00	1.00
2002				1.00	1.00	1.00
2005					1.00	1.00
2006						1.00

Bigeye in the eastern central Atlantic

2004 2013 2014 2015 2016 2019
2020 2021 2022

<i>2003</i>	1.00	1.00	1.00	1.00	0.28	< 0.05	1.00	0.48	1.00
<i>2004</i>		1.00	1.00	1.00	0.52	< 0.05	1.00	0.83	1.00
<i>2013</i>			1.00	1.00	1.00	0.61	1.00	1.00	1.00
<i>2014</i>				1.00	0.21	< 0.05	1.00	0.23	1.00
<i>2015</i>					1.00	< 0.05	1.00	1.00	1.00
<i>2016</i>						1.00	0.24	1.00	1.00
<i>2019</i>							< 0.05	1.00	0.97
<i>2020</i>								0.31	1.00
<i>2021</i>									1.00

Table S4. Year-to-year comparisons of tuna nitrogen isotope values. Results of the post-hoc Dunn's tests on $\delta^{15}\text{N}$ values measured in muscle tissues of **A**) yellowfin, **B**) bigeye, and **C**) skipjack in the southwestern Pacific, **D**) yellowfin, **E**) bigeye, and **F**) skipjack in the western Indian, and **G**) yellowfin and **H**) bigeye in the eastern central Pacific.

A)Yellowfin in the southwestern Pacific

2003	2004	2005	2006	2007	2008	2009	2010	2011	2013	2014	2015	2016	2017	2018	2020
------	------	------	------	------	------	------	------	------	------	------	------	------	------	------	------

2001	< 0.05	1.00	1.00	< 0.05	< 0.05	< 0.05	1.00	1.00	< 0.05	0.32	1.00	< 0.05	1.00	< 0.05	1.00
2003															
2004		1.00	0.83	1.00	1.00	1.00	1.00	1.00	1.00	1.00	1.00	1.00	1.00	1.00	0.13
2005															
2006				1.00	1.00	1.00	< 0.05	1.00	1.00	1.00	1.00	1.00	1.00	1.00	1.00
2007							< 0.05	< 0.05	0.17	< 0.05	1.00	1.00	< 0.05	1.00	1.00
2008									1.00	1.00	1.00	0.31	1.00	0.33	0.49
2009										1.00	1.00	1.00	1.00	0.08	1.00
2010											1.00	0.15	< 0.05	0.38	< 0.05
2011												1.00	1.00	1.00	< 0.05
2013												1.00	1.00	1.00	< 0.05
2014													1.00	< 0.05	0.07
2015													< 0.05	< 0.05	< 0.05
2016														1.00	1.00
2017														1.00	1.00
2018														0.40	1.00
B)															
Bigeye in the															
														0.12	1.00
														1.00	0.79
														1.00	1.00
														0.20	1.00
														1.00	1.00
															0.27

southwestern Pacific

2003 2007 2008 2009 2011 2013 2014 2015 2017 2018 2021

2001	0.11	< 0.05	< 0.05	1.00	1.00	< 0.05	0.38	< 0.05	1.00	< 0.05	0.22
2003		1.00	1.00	1.00	1.00	1.00	1.00	1.00	1.00	1.00	1.00
2007			1.00	< 0.05	< 0.05	1.00	< 0.05	< 0.05	< 0.05	1.00	0.48
2009				0.08	0.11	1.00	0.60	0.86	0.18	1.00	1.00
2011					1.00	0.16	1.00	1.00	1.00	1.00	1.00
2013						0.75	1.00	1.00	1.00	1.00	1.00
2014							1.00	1.00	1.00	1.00	1.00
2015								1.00	1.00	1.00	1.00
2017									1.00	1.00	1.00
2018										1.00	1.00
											1.00

C) Skipjack in the southwestern Pacific

	2003	2004	2007	2008	2009	2010	2013	2014	2015	2016	2017	2018	2020	2021
2001	1.00	1.00	1.00	1.00	1.00	1.00	1.00	1.00	1.00	1.00	1.00	1.00	1.00	1.00
2003		1.00	0.27	1.00	1.00	1.00	1.00	1.00	0.05	0.20	1.00	1.00	1.00	1.00
2004			1.00	1.00	1.00	1.00	1.00	1.00	1.00	1.00	1.00	1.00	1.00	1.00
2007				1.00	1.00	1.00	1.00	1.00	1.00	1.00	1.00	1.00	1.00	1.00
2008					1.00	1.00	1.00	< 0.05	1.00	1.00	1.00	1.00	0.63	0.15
2009						1.00	1.00	1.00	1.00	1.00	1.00	1.00		
2010							1.00	1.00	1.00	1.00	1.00	1.00	1.00	1.00
2013								1.00	1.00	1.00	1.00	1.00	1.00	1.00
2014								1.00	1.00	1.00	1.00	1.00	1.00	1.00
2015									1.00	1.00	1.00	1.00	1.00	1.00
2016									0.62	1.00	1.00	1.00	1.00	1.00
2017										1.00	1.00	1.00	1.00	1.00
2018										0.31	1.00	1.00	1.00	1.00
2020											< 0.05	< 0.05	1.00	1.00
D)												1.00	1.00	0.24
												1.00	1.00	0.05
												1.00	1.00	
												1.00	1.00	
												1.00	1.00	
													1.00	

Yellowfin in the western Indian

2003 2004 2010 2011 2012 2013 2014 2015 2017 2018 2020 2022

2001	1.00	< 0.05	1.00	1.00	1.00	< 0.05	1.00	1.00	1.00	< 0.05	0.27	1.00
2003		1.00	1.00	1.00	1.00	1.00	1.00	1.00	1.00	1.00	1.00	1.00
2004			1.00	1.00	0.64	1.00	1.00	1.00	0.11	1.00	1.00	1.00
2010				1.00	1.00	1.00	1.00	1.00	1.00	1.00	1.00	1.00
2011					1.00	1.00	1.00	1.00	1.00	1.00	1.00	1.00
2012						1.00	1.00	1.00	1.00	1.00	1.00	1.00
2013							1.00	1.00	1.00	1.00	1.00	1.00
2014								0.58	1.00	1.00	0.41	1.00
2015									1.00	1.00	1.00	1.00
2017										0.05	1.00	1.00
2018											1.00	1.00
2020											1.00	1.00
E) Bigeye in the western Indian												

2002

2011

2012

2013

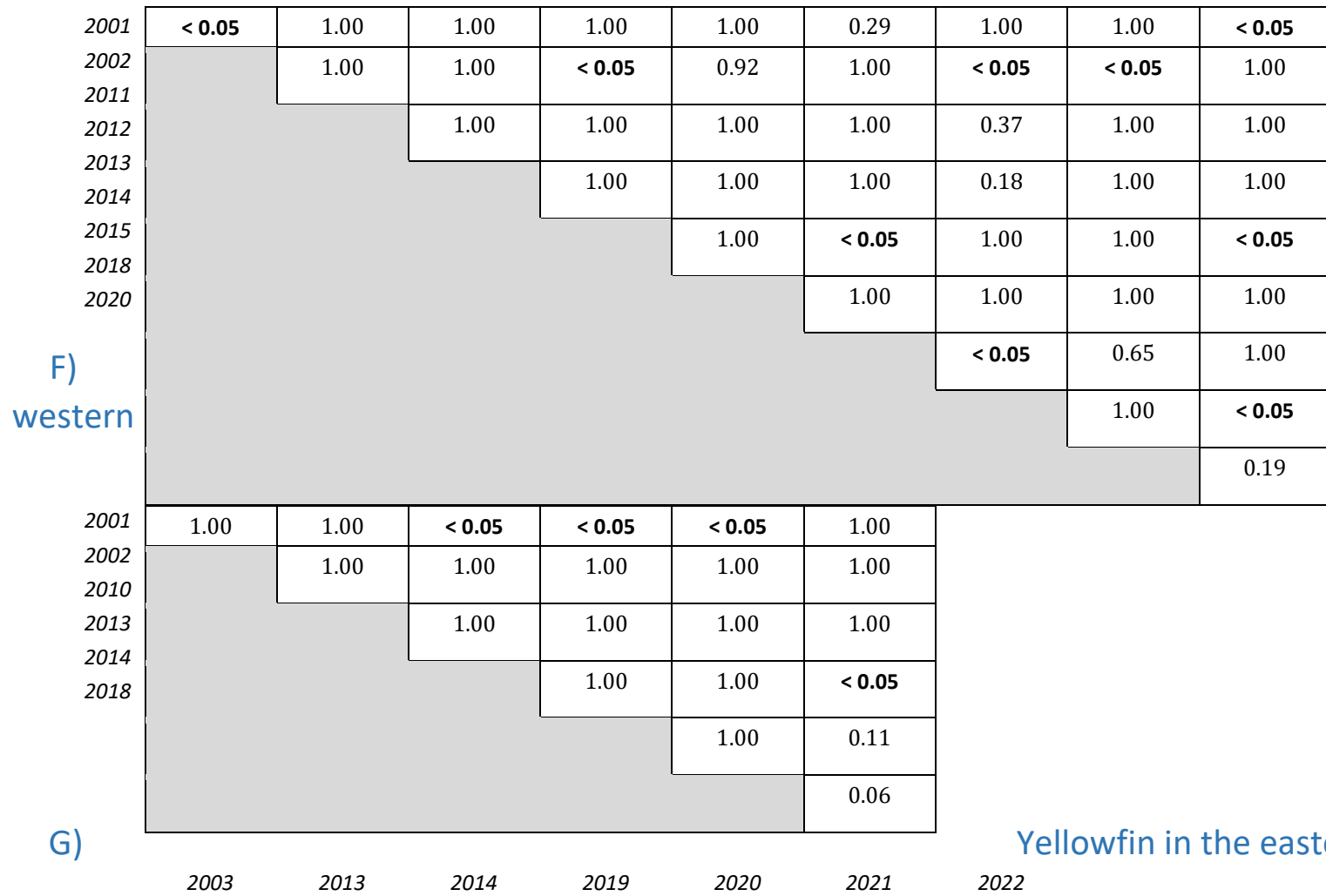
2014

2015

2018

2020

2022



Skipjack in the Indian

2002 2010 2013
2014 2018 2022

Yellowfin in the eastern central Atlantic

H) Atlantic

2002	1.00	1.00	1.00	1.00	1.00	1.00
2003		< 0.05	< 0.05	< 0.05	< 0.05	< 0.05
2013						
2014		1.00	1.00	1.00	1.00	1.00
2019						
2020			1.00	1.00	1.00	1.00
2021				1.00	1.00	1.00
					1.00	1.00
ntic						1.00

Bigeye in the eastern central

2004 2013 2014 2015 2016

References used in the document

- (1) Boush, G. M.; Thieleke, J. R. Total Mercury Content in Yellowfin and Bigeye Tuna. *Bull. Environ. Contam. Toxicol.* **1983**, *30* (1), 291–297. <https://doi.org/10.1007/BF01610135>.
- (2) Brooks, B. Mercury Levels in Tuna and Other Major Commercial Fish Species in Hawaii; San Diego, CA, USA, 2004; p 24.
- (3) Ivory Coast Fisheries Service. *La Contamination Mercurielle Des Thons. Mercury Contamination in Tuna Fish*; Abidjan, 1972; p 5.
- (4) Kaneko, J. J.; Ralston, N. V. C. Selenium and Mercury in Pelagic Fish in the Central North Pacific Near Hawaii. *Biol Trace Elem Res* **2007**, *119* (3), 242–254. <https://doi.org/10.1007/s12011-0078004-8>.
- (5) Kraepiel, A. M. L.; Keller, K.; Chin, H. B.; Malcolm, E. G.; Morel, F. M. M. Sources and Variations of Mercury in Tuna. *Environmental Science & Technology* **2003**, *37* (24), 5551–5558. <https://doi.org/10.1021/es0340679>.
- (6) Rivers, J. B.; Pearson, J. E.; Shultz, C. D. Total and Organic Mercury in Marine Fish. *Bull. Environ. Contam. Toxicol.* **1972**, *8* (5), 257–266. <https://doi.org/10.1007/BF01684554>.
- (7) Drevnick, P. E.; Brooks, B. A. Mercury in Tunas and Blue Marlin in the North Pacific Ocean. *Environmental Toxicology and Chemistry* **2017**, *36* (5), 1365–1374. <https://doi.org/10.1002/etc.3757>.
- (8) Peterson, C. L.; Klawe, W. L.; Sharp, G. D. Mercury in Tunas: A Review. *Fishery Bulletin* **1973**, *71* (3), 11.
- (9) Adams, D. H. Total Mercury Levels in Tunas from Offshore Waters of the Florida Atlantic Coast. *Marine Pollution Bulletin* **2004**, *49* (7–8), 659–663. <https://doi.org/10.1016/j.marpolbul.2004.06.005>.
- (10) Blum, J. D.; Popp, B. N.; Drazen, J. C.; Anela Choy, C.; Johnson, M. W. Methylmercury Production below the Mixed Layer in the North Pacific Ocean. *Nature Geoscience* **2013**, *6* (10), 879–884. <https://doi.org/10.1038/ngeo1918>.
- (11) Choy, C. A.; Popp, B. N.; Kaneko, J. J.; Drazen, J. C. The Influence of Depth on Mercury Levels in Pelagic Fishes and Their Prey. *Proceedings of the National Academy of Sciences* **2009**, *106* (33), 13865–13869. <https://doi.org/10.1073/pnas.0900711106>.
- (12) Ferriss, B. E.; Essington, T. E. Regional Patterns in Mercury and Selenium Concentrations of Yellowfin Tuna (*Thunnus Albacares*) and Bigeye Tuna (*Thunnus Obesus*) in the Pacific Ocean. *Can. J. Fish. Aquat. Sci.* **2011**, *68* (12), 2046–2056. <https://doi.org/10.1139/f2011-120>.
- (13) Kojadinovic, J.; Potier, M.; Le Corre, M.; Cosson, R. P.; Bustamante, P. Mercury Content in Commercial Pelagic Fish and Its Risk Assessment in the Western Indian Ocean. *Science of The Total Environment* **2006**, *366* (2–3), 688–700. <https://doi.org/10.1016/j.scitotenv.2006.02.006>.
- (14) Médieu, A.; Point, D.; Receveur, A.; Gauthier, O.; Allain, V.; Pethybridge, H.; Menkes, C. E.; Gillikin, D. P.; Revill, A. T.; Somes, C. J.; Collin, J.; Lorrain, A. Stable Mercury Concentrations of Tropical Tuna in the South Western Pacific Ocean: An 18-Year Monitoring Study. *Chemosphere* **2021**, *263*, 128024. <https://doi.org/10.1016/j.chemosphere.2020.128024>.
- (15) Chassot, E. *A Review of Morphometric Data Available for Tropical Tunas: Updating Relationships for Purse Seine Fisheries Data Processing*; working document; IRD, Ob7, 2015.
- (16) Macdonald, J.; Williams, P.; Sanchez, C.; Schneiter, E.; Prasad, S.; Ghergariu, M.; Hosken, M.; Panizza, A.; Park, T.; Guillou, A.; Nicol, S. Project 90 Update: Better Data on Fish Weights and Lengths for Scientific Analyses; 2022.
- (17) Médieu, A.; Point, D.; Itai, T.; Angot, H.; Buchanan, P. J.; Allain, V.; Fuller, L.; Griffiths, S.; Gillikin, D. P.; Sonke, J. E.; Heimbürger-Boavida, L.-E.; Desgranges, M.-M.; Menkes, C. E.; Madigan, D. J.;

Brosset, P.; Gauthier, O.; Tagliabue, A.; Bopp, L.; Verheyden, A.; Lorrain, A. Evidence That Pacific Tuna Mercury Levels Are Driven by Marine Methylmercury Production and Anthropogenic Inputs. *PNAS* **2022**, *119* (2), 8. <https://doi.org/10.1073/pnas.2113032119>.

- (18) Médieau, A.; Sardenne, F.; Lorrain, A.; Bodin, N.; Pazart, C.; Le Delliou, H.; Point, D. Lipid-Free Tuna Muscle Samples Are Suitable for Total Mercury Analysis. *Marine Environmental Research* **2021**, *169*, 105385. <https://doi.org/10.1016/j.marenvres.2021.105385>.
- (19) Médieau, A.; Lorrain, A.; Point, D. Are Tunas Relevant Bioindicators of Mercury Concentrations in the Global Ocean? *Ecotoxicology* **2023**. <https://doi.org/10.1007/s10646-023-02679-y>.
- (20) Fry, B. *Stable Isotope Ecology*; Springer: New York, NY, 2006.
- (21) Sardenne, F.; Bodin, N.; Chassot, E.; Amiel, A.; Fouché, E.; Degroote, M.; Hollanda, S.; Pethybridge, H.; Lebreton, B.; Guillou, G.; Ménard, F. Trophic Niches of Sympatric Tropical Tuna in the Western Indian Ocean Inferred by Stable Isotopes and Neutral Fatty Acids. *Progress in Oceanography* **2016**, *146*, 75–88. <https://doi.org/10.1016/j.pocean.2016.06.001>.
- (22) Sardenne, F.; Diaha, N. C.; Amandé, M. J.; Zudaire, I.; Couturier, L. I. E.; Metral, L.; Le Grand, F.; Bodin, N. Seasonal Habitat and Length Influence on the Trophic Niche of Co-Occurring Tropical Tunas in the Eastern Atlantic Ocean. *Can. J. Fish. Aquat. Sci.* **2019**, *76* (1), 69–80. <https://doi.org/10.1139/cjfas-2017-0368>.
- (23) Ménard, F.; Lorrain, A.; Potier, M.; Marsac, F. Isotopic Evidence of Distinct Feeding Ecologies and Movement Patterns in Two Migratory Predators (Yellowfin Tuna and Swordfish) of the Western Indian Ocean. *Marine Biology* **2007**, *153* (2), 141–152. <https://doi.org/10.1007/s00227-007-0789-7>.
- (24) Logan, J. M.; Jardine, T. D.; Miller, T. J.; Bunn, S. E.; Cunjak, R. A.; Lutcavage, M. E. Lipid Corrections in Carbon and Nitrogen Stable Isotope Analyses: Comparison of Chemical Extraction and Modelling Methods. *Journal of Animal Ecology* **2008**, *77* (4), 838–846. <https://doi.org/10.1111/j.1365-2656.2008.01394.x>.
- (25) Amos, H. M.; Jacob, D. J.; Kocman, D.; Horowitz, H. M.; Zhang, Y.; Dutkiewicz, S.; Horvat, M.; Corbitt, E. S.; Krabbenhoft, D. P.; Sunderland, E. M. Global Biogeochemical Implications of Mercury Discharges from Rivers and Sediment Burial. *Environ. Sci. Technol.* **2014**, *48* (16), 9514–9522. <https://doi.org/10.1021/es502134t>.
- (26) Amos, H. M.; Jacob, D. J.; Streets, D. G.; Sunderland, E. M. Legacy Impacts of All-Time Anthropogenic Emissions on the Global Mercury Cycle. *Global Biogeochemical Cycles* **2013**, *27* (2), 410–421. <https://doi.org/10.1002/gbc.20040>.
- (27) Streets, D. G.; Horowitz, H. M.; Lu, Z.; Levin, L.; Thackray, C. P.; Sunderland, E. M. Global and Regional Trends in Mercury Emissions and Concentrations, 2010–2015. *Atmospheric Environment* **2019**, *201*, 417–427. <https://doi.org/10.1016/j.atmosenv.2018.12.031>.
- (28) Streets, D. G.; Horowitz, H. M.; Lu, Z.; Levin, L.; Thackray, C. P.; Sunderland, E. M. Five Hundred Years of Anthropogenic Mercury: Spatial and Temporal Release Profiles. *Environ. Res. Lett.* **2019**, *14* (8), 084004. <https://doi.org/10.1088/1748-9326/ab281f>.
- (29) Streets, D. G.; Horowitz, H. M.; Jacob, D. J.; Lu, Z.; Levin, L.; ter Schure, A. F. H.; Sunderland, E. M. Total Mercury Released to the Environment by Human Activities. *Environ. Sci. Technol.* **2017**, *51* (11), 5969–5977. <https://doi.org/10.1021/acs.est.7b00451>.
- (30) Streets, D. G.; Devane, M. K.; Lu, Z.; Bond, T. C.; Sunderland, E. M.; Jacob, D. J. All-Time Releases of Mercury to the Atmosphere from Human Activities. *Environmental Science & Technology* **2011**, *45* (24), 10485–10491. <https://doi.org/10.1021/es202765m>.

- (31) Angot, H.; Hoffman, N.; Giang, A.; Thackray, C. P.; Hendricks, A. N.; Urban, N. R.; Selin, N. E. Global and Local Impacts of Delayed Mercury Mitigation Efforts. *Environ. Sci. Technol.* **2018**, *52* (22), 12968–12977. <https://doi.org/10.1021/acs.est.8b04542>.
- (32) Pacyna, J. M.; Travnikov, O.; De Simone, F.; Hedgecock, I. M.; Sundseth, K.; Pacyna, E. G.; Steenhuisen, F.; Pirrone, N.; Munthe, J.; Kindbom, K. Current and Future Levels of Mercury Atmospheric Pollution on a Global Scale. *Atmospheric Chemistry and Physics* **2016**, *16* (19), 12495–12511. <https://doi.org/10.5194/acp-16-12495-2016>.
- (33) Masbou, J.; Point, D.; Sonke, J. E.; Frappart, F.; Perrot, V.; Amouroux, D.; Richard, P.; Becker, P. R. Hg Stable Isotope Time Trend in Ringed Seals Registers Decreasing Sea Ice Cover in the Alaskan Arctic. *Environ. Sci. Technol.* **2015**, *49* (15), 8977–8985. <https://doi.org/10.1021/es5048446>.
- (34) Morris, A. D.; Wilson, S. J.; Fryer, R. J.; Thomas, P. J.; Hudelson, K.; Andreasen, B.; Blévin, P.; Bustamante, P.; Chastel, O.; Christensen, G.; Dietz, R.; Evans, M.; Evenset, A.; Ferguson, S. H.; Fort, J.; Gamberg, M.; Grémillet, D.; Houde, M.; Letcher, R. J.; Loseto, L.; Muir, D.; Pinzone, M.; Poste, A.; Routti, H.; Sonne, C.; Stern, G.; Rigét, F. F. Temporal Trends of Mercury in Arctic Biota: 10 More Years of Progress in Arctic Monitoring. *Science of The Total Environment* **2022**, *839*, 155803. <https://doi.org/10.1016/j.scitotenv.2022.155803>.
- (35) Bignert, A.; Riget, F.; Braune, B.; Outridge, P.; Wilson, S. Recent Temporal Trend Monitoring of Mercury in Arctic Biota – How Powerful Are the Existing Data Sets? *J. Environ. Monit.* **2004**, *6* (4), 351–355. <https://doi.org/10.1039/B312118F>.
- (36) Bignert, A. *PIA Statistical Application Developed for Use by the Arctic Monitoring and Assessment Programme*; Arctic Monitoring and Assessment Programme, 2007; p 13.
- (37) *MATLAB Documentation - MathWorks United Kingdom*. <https://uk.mathworks.com/help/matlab/> (accessed 2023-09-04).
- (38) R Core Team. *R: A Language and Environment for Statistical Computing*; 2015; Vienna, Austria, 2018.
- (39) Aumont, O.; Ethé, C.; Tagliabue, A.; Bopp, L.; Gehlen, M. PISCES-v2: An Ocean Biogeochemical Model for Carbon and Ecosystem Studies. *Geosci. Model Dev.* **2015**, *8* (8), 2465–2513. <https://doi.org/10.5194/gmd-8-2465-2015>.
- (40) Lorrain, A.; Pethybridge, H.; Cassar, N.; Receveur, A.; Allain, V.; Bodin, N.; Bopp, L.; Choy, C. A.; Duffy, L.; Fry, B.; Goñi, N.; Graham, B. S.; Hobday, A. J.; Logan, J. M.; Ménard, F.; Menkes, C. E.; Olson, R. J.; Pagendam, D. E.; Point, D.; Revill, A. T.; Somes, C. J.; Young, J. W. Trends in Tuna Carbon Isotopes Suggest Global Changes in Pelagic Phytoplankton Communities. *Glob Change Biol* **2020**, *26* (2), 458–470. <https://doi.org/10.1111/gcb.14858>.
- (41) AMAP; UN Environment. *Technical Background Report for the Global Mercury Assessment 2018. Arctic Monitoring and Assessment Programme, Oslo, Norway/UN Environment Programme, Chemicals and Health Branch*; Geneva, Switzerland, 2019; p viii + 426 pp including E-Annexes.
- (42) Skov, H.; Hjorth, J.; Nordstrøm, C.; Jensen, B.; Christoffersen, C.; Bech Poulsen, M.; Baldtzer Liisberg, J.; Beddows, D.; Dall’Osto, M.; Christensen, J. H. Variability in Gaseous Elemental Mercury at Villum Research Station, Station Nord, in North Greenland from 1999 to 2017. *Atmospheric Chemistry and Physics* **2020**, *20* (21), 13253–13265. <https://doi.org/10.5194/acp20-13253-2020>.
- (43) MacSween, K.; Stupple, G.; Aas, W.; Kyllönen, K.; Pfaffhuber, K. A.; Skov, H.; Steffen, A.; Berg, T.; Mastromonaco, M. N. Updated Trends for Atmospheric Mercury in the Arctic: 1995–2018. *Science of The Total Environment* **2022**, *837*, 155802. <https://doi.org/10.1016/j.scitotenv.2022.155802>.

- (44) Berg, T.; Bartnicki, J.; Munthe, J.; Lattila, H.; Hrehoruk, J.; Mazur, A. Atmospheric Mercury Species in the European Arctic: Measurements and Modelling. *Atmospheric Environment* **2001**, *35* (14), 2569–2582. [https://doi.org/10.1016/S1352-2310\(00\)00434-9](https://doi.org/10.1016/S1352-2310(00)00434-9).
- (45) Sprovieri, F.; Pirrone, N.; Bencardino, M.; D'Amore, F.; Carbone, F.; Cinnirella, S.; Mannarino, V.; Landis, M.; Ebinghaus, R.; Weigelt, A.; Brunke, E.-G.; Labuschagne, C.; Martin, L.; Munthe, J.; Wängberg, I.; Artaxo, P.; Morais, F.; Barbosa, H. de M. J.; Brito, J.; Cairns, W.; Barbante, C.; Diéguez, M. del C.; Garcia, P. E.; Dommergue, A.; Angot, H.; Magand, O.; Skov, H.; Horvat, M.; Kotnik, J.; Read, K. A.; Neves, L. M.; Gawlik, B. M.; Sena, F.; Mashyanov, N.; Obolkin, V.; Wip, D.; Feng, X. B.; Zhang, H.; Fu, X.; Ramachandran, R.; Cossa, D.; Knoery, J.; Marusczak, N.; Nerentorp, M.; Norstrom, C. Atmospheric Mercury Concentrations Observed at Ground-Based Monitoring Sites Globally Distributed in the Framework of the GMOS Network. *Atmospheric Chemistry and Physics* **2016**, *16* (18), 11915–11935. <https://doi.org/10.5194/acp-16-11915-2016>.
- (46) Custódio, A.; Pfaffhuber, K. A.; Spain, T. G.; Pankratov, F. F.; Strigunova, I.; Molepo, K.; Skov, H.; Bieser, J.; Ebinghaus, R. Odds and Ends of Atmospheric Mercury in Europe and over the North Atlantic Ocean: Temporal Trends of 25 Years of Measurements. *Atmospheric Chemistry and Physics* **2022**, *22*, 3827–3840. <https://doi.org/10.5194/acp-22-3827-2022>.
- (47) Angot, H.; Barret, M.; Magand, O.; Ramonet, M.; Dommergue, A. A 2-Year Record of Atmospheric Mercury Species at a Background Southern Hemisphere Station on Amsterdam Island. *Atmospheric Chemistry and Physics* **2014**, *14* (20), 11461–11473. <https://doi.org/10.5194/acp-14-11461-2014>.
- (48) Magand, O.; Angot, H.; Bertrand, Y.; Sonke, J. E.; Laffont, L.; Duperray, S.; Collignon, L.; Boulanger, D.; Dommergue, A. Over a Decade of Atmospheric Mercury Monitoring at Amsterdam Island in the French Southern and Antarctic Lands. *Sci Data* **2023**, *10* (1), 836. <https://doi.org/10.1038/s41597-023-02740-9>.
- (49) Slemr, F.; Martin, L.; Labuschagne, C.; Mkhololo, T.; Angot, H.; Magand, O.; Dommergue, A.; Garat, P.; Ramonet, M.; Bieser, J. Atmospheric Mercury in the Southern Hemisphere – Part 1: Trend and Inter-Annual Variations in Atmospheric Mercury at Cape Point, South Africa, in 2007–2017, and on Amsterdam Island in 2012–2017. *Atmos. Chem. Phys.* **2020**, *20* (13), 7683–7692. <https://doi.org/10.5194/acp-20-7683-2020>.
- (50) Slemr, F.; Angot, H.; Dommergue, A.; Magand, O.; Barret, M.; Weigelt, A.; Ebinghaus, R.; Brunke, E.-G.; Pfaffhuber, K. A.; Edwards, G.; Howard, D.; Powell, J.; Keywood, M.; Wang, F. Comparison of Mercury Concentrations Measured at Several Sites in the Southern Hemisphere. *Atmospheric Chemistry and Physics* **2015**, *15* (6), 3125–3133. <https://doi.org/10.5194/acp-153125-2015>.
- (51) Martin, L. G.; Labuschagne, C.; Brunke, E.-G.; Weigelt, A.; Ebinghaus, R.; Slemr, F. Trend of Atmospheric Mercury Concentrations at Cape Point for 1995–2004 and since 2007. *Atmospheric Chemistry and Physics* **2017**, *17* (3), 2393–2399. <https://doi.org/10.5194/acp-172393-2017>.
- (52) Diéguez, M. C.; Bencardino, M.; García, P. E.; D'Amore, F.; Castagna, J.; De Simone, F.; Soto Cárdenas, C.; Ribeiro Guevara, S.; Pirrone, N.; Sprovieri, F. A Multi-Year Record of Atmospheric

Mercury Species at a Background Mountain Station in Andean Patagonia (Argentina): Temporal Trends and Meteorological Influence. *Atmospheric Environment* **2019**, *214*, 116819.
<https://doi.org/10.1016/j.atmosenv.2019.116819>.

- (53) Angot, H.; Dastoor, A.; De Simone, F.; Gårdfeldt, K.; Gencarelli, C. N.; Hedgecock, I. M.; Langer, S.; Magand, O.; Mastromonaco, M. N.; Nordstrøm, C.; Pfaffhuber, K. A.; Pirrone, N.; Ryjkov, A.; Selin, N. E.; Skov, H.; Song, S.; Sprovieri, F.; Steffen, A.; Toyota, K.; Travnikov, O.; Yang, X.; Dommergue, A. Chemical Cycling and Deposition of Atmospheric Mercury in Polar Regions: Review of Recent Measurements and Comparison with Models. *Atmospheric Chemistry and Physics* **2016**, *16* (16), 10735–10763. <https://doi.org/10.5194/acp-16-10735-2016>.
- (54) Angot, H.; Dion, I.; Vogel, N.; Legrand, M.; Magand, O.; Dommergue, A. Multi-Year Record of Atmospheric Mercury at Dumont d'Urville, East Antarctic Coast: Continental Outflow and Oceanic Influences. *Atmospheric Chemistry and Physics* **2016**, *16* (13), 8265–8279.
<https://doi.org/10.5194/acp-16-8265-2016>.
- (55) Angot, H.; Magand, O.; Helmig, D.; Ricaud, P.; Quennehen, B.; Gallée, H.; Del Guasta, M.; Sprovieri, F.; Pirrone, N.; Savarino, J.; Dommergue, A. New Insights into the Atmospheric Mercury Cycling in Central Antarctica and Implications on a Continental Scale. *Atmospheric Chemistry and Physics* **2016**, *16* (13), 8249–8264. <https://doi.org/10.5194/acp-16-8249-2016>.
- (56) Gay, D. A.; Schmelz, D.; Prestbo, E.; Olson, M.; Sharac, T.; Tordon, R. The Atmospheric Mercury Network: Measurement and Initial Examination of an Ongoing Atmospheric Mercury Record across North America. *Atmospheric Chemistry and Physics* **2013**, *13* (22), 11339–11349.
<https://doi.org/10.5194/acp-13-11339-2013>.
- (57) Fraser, A.; Dastoor, A.; Ryjkov, A. How Important Is Biomass Burning in Canada to Mercury Contamination? *Atmospheric Chemistry and Physics* **2018**, *18* (10), 7263–7286.
<https://doi.org/10.5194/acp-18-7263-2018>.
- (58) Foley, T. A.; Kenski, D. Total Gaseous Mercury (TGM) Concentration over Lake Superior and Lake Michigan. *Journal of Great Lakes Research* **2021**, *47* (5), 1345–1357.
<https://doi.org/10.1016/j.jglr.2021.06.003>.
- (59) Mao, H.; Ye, Z.; Driscoll, C. Meteorological Effects on Hg Wet Deposition in a Forested Site in the Adirondack Region of New York during 2000–2015. *Atmospheric Environment* **2017**, *168*, 90–100. <https://doi.org/10.1016/j.atmosenv.2017.08.058>.
- (60) Choi, H.-D.; Holsen, T. M.; Hopke, P. K. Atmospheric Mercury (Hg) in the Adirondacks: Concentrations and Sources. *Environ. Sci. Technol.* **2008**, *42* (15), 5644–5653.
<https://doi.org/10.1021/es7028137>.
- (61) Zhou, H.; Hopke, P. K.; Zhou, C.; Holsen, T. M. Ambient Mercury Source Identification at a New York State Urban Site: Rochester, NY. *Science of The Total Environment* **2019**, *650*, 1327–1337.
<https://doi.org/10.1016/j.scitotenv.2018.09.040>.
- (62) Yatavelli, R. L. N.; Fahrni, J. K.; Kim, M.; Crist, K. C.; Vickers, C. D.; Winter, S. E.; Connell, D. P. Mercury, PM_{2.5} and Gaseous Co-Pollutants in the Ohio River Valley Region: Preliminary Results from the Athens Supersite. *Atmospheric Environment* **2006**, *40* (34), 6650–6665.
<https://doi.org/10.1016/j.atmosenv.2006.05.072>.
- (63) Cole, A. S.; Steffen, A.; Eckley, C. S.; Narayan, J.; Pilote, M.; Tordon, R.; Graydon, J. A.; St. Louis, V. L.; Xu, X.; Branfireun, B. A. A Survey of Mercury in Air and Precipitation across Canada: Patterns and Trends. *Atmosphere* **2014**, *5* (3), 635–668.
<https://doi.org/10.3390/atmos5030635>.

- (64) Dastoor, A.; Ryjkov, A.; Kos, G.; Zhang, J.; Kirk, J.; Parsons, M.; Steffen, A. Impact of Athabasca Oil Sands Operations on Mercury Levels in Air and Deposition. *Atmospheric Chemistry and Physics* **2021**, *21* (16), 12783–12807. <https://doi.org/10.5194/acp-21-12783-2021>.
- (65) Nguyen, H. T.; Kim, K.-H.; Kim, M.-Y.; Hong, S.; Youn, Y.-H.; Shon, Z.-H.; Lee, J. S. Monitoring of Atmospheric Mercury at a Global Atmospheric Watch (GAW) Site on An-Myun Island, Korea. *Water Air Soil Pollut* **2007**, *185* (1), 149–164. <https://doi.org/10.1007/s11270-007-9438-5>.
- (66) Marumoto, K.; Suzuki, N.; Shibata, Y.; Takeuchi, A.; Takami, A.; Fukuzaki, N.; Kawamoto, K.; Mizohata, A.; Kato, S.; Yamamoto, T.; Chen, J.; Hattori, T.; Nagasaka, H.; Saito, M. Long-Term Observation of Atmospheric Speciated Mercury during 2007–2018 at Cape Hedo, Okinawa, Japan. *Atmosphere* **2019**, *10* (7), 362. <https://doi.org/10.3390/atmos10070362>.
- (67) Yang, Y.; Chen, H.; Wang, D. Spatial and Temporal Distribution of Gaseous Elemental Mercury in Chongqing, China. *Environ Monit Assess* **2009**, *156* (1), 479–489. <https://doi.org/10.1007/s10661-008-0499-8>.
- (68) Fu, X. W.; Zhang, H.; Yu, B.; Wang, X.; Lin, C.-J.; Feng, X. B. Observations of Atmospheric Mercury in China: A Critical Review. *Atmos. Chem. Phys.* **2015**, *15* (16), 9455–9476. <https://doi.org/10.5194/acp-15-9455-2015>.
- (69) Nguyen, H. T.; Kim, M.-Y.; Kim, K.-H. The Influence of Long-Range Transport on Atmospheric Mercury on Jeju Island, Korea. *Science of The Total Environment* **2010**, *408* (6), 1295–1307. <https://doi.org/10.1016/j.scitotenv.2009.10.029>.
- (70) Nguyen, L. S. P.; Sheu, G.-R.; Lin, D.-W.; Lin, N.-H. Temporal Changes in Atmospheric Mercury Concentrations at a Background Mountain Site Downwind of the East Asia Continent in 2006–2016. *Science of The Total Environment* **2019**, *686*, 1049–1056. <https://doi.org/10.1016/j.scitotenv.2019.05.425>.
- (71) Fu, X.; Feng, X.; Sommar, J.; Wang, S. A Review of Studies on Atmospheric Mercury in China. *Science of The Total Environment* **2012**, *421–422*, 73–81. <https://doi.org/10.1016/j.scitotenv.2011.09.089>.
- (72) Kim, K.-H.; Brown, R. J. C.; Kwon, E.; Kim, I.-S.; Sohn, J.-R. Atmospheric Mercury at an Urban Station in Korea across Three Decades. *Atmospheric Environment* **2016**, *131*, 124–132. <https://doi.org/10.1016/j.atmosenv.2016.01.051>.
- (73) Osawa, T.; Ueno, T.; Fu, F. Sequential Variation of Atmospheric Mercury in Tokai-Mura, Seaside Area of Eastern Central Japan. *Journal of Geophysical Research: Atmospheres* **2007**, *112* (D19). <https://doi.org/10.1029/2007JD008538>.
- (74) Shi, J.; Chen, Y.; Xu, L.; Hong, Y.; Li, M.; Fan, X.; Yin, L.; Chen, Y.; Yang, C.; Chen, G.; Liu, T.; Ji, X.; Chen, J. Measurement Report: Atmospheric Mercury in a Coastal City of Southeast China – Inter-Annual Variations and Influencing Factors. *Atmospheric Chemistry and Physics* **2022**, *22* (17), 11187–11202. <https://doi.org/10.5194/acp-22-11187-2022>.
- (75) Lee, G.-S.; Kim, P.-R.; Han, Y.-J.; Holsen, T. M.; Seo, Y.-S.; Yi, S.-M. Atmospheric Speciated Mercury Concentrations on an Island between China and Korea: Sources and Transport Pathways. *Atmospheric Chemistry and Physics* **2016**, *16* (6), 4119–4133. <https://doi.org/10.5194/acp-16-4119-2016>.
- (76) Kentisbeer, J.; Leeson, S. R.; Clark, T.; Malcolm, H. M.; Cape, J. N. Correction: Influences on and Patterns in Total Gaseous Mercury (TGM) at Harwell, England. *Environ. Sci.: Processes Impacts* **2015**, *17* (3), 700–700. <https://doi.org/10.1039/C5EM90005K>.

- (77) Kentisbeer, J.; Leeson, S. R.; Malcolm, H. M.; Leith, I. D.; Braban, C. F.; Cape, J. N. Patterns and Source Analysis for Atmospheric Mercury at Auchencorth Moss, Scotland. *Environ. Sci.: Processes Impacts* **2014**, *16* (5), 1112–1123. <https://doi.org/10.1039/C3EM00700F>.
- (78) Howard, D.; Nelson, P. F.; Edwards, G. C.; Morrison, A. L.; Fisher, J. A.; Ward, J.; Harnwell, J.; van der Schoot, M.; Atkinson, B.; Chambers, S. D.; Griffiths, A. D.; Werczynski, S.; Williams, A. G. Atmospheric Mercury in the Southern Hemisphere Tropics: Seasonal and Diurnal Variations and Influence of Inter-Hemispheric Transport. *Atmospheric Chemistry and Physics* **2017**, *17* (18), 11623–11636. <https://doi.org/10.5194/acp-17-11623-2017>.
- (79) Koenig, A. M.; Magand, O.; Verreyken, B.; Brioude, J.; Amelynck, C.; Schoon, N.; Colomb, A.; Ferreira Araujo, B.; Ramonet, M.; Sha, M. K.; Cammas, J.-P.; Sonke, J. E.; Dommergue, A. Mercury in the Free Troposphere and Bidirectional Atmosphere–Vegetation Exchanges – Insights from Maïdo Mountain Observatory in the Southern Hemisphere Tropics. *Atmospheric Chemistry and Physics* **2023**, *23* (2), 1309–1328. <https://doi.org/10.5194/acp-23-1309-2023>.